Optimum sustainable distributed hybrid generation using forecasting and multi-criteria decision making: demonstration for an Indian village

A THESIS SUBMITTED TOWARDS PARTIAL FULFILMENT OF THE REQUIREMENTS FOR THE DEGREE OF

Master of Technology
In
Energy Science and Technology

Course Affiliated To
Faculty of Engineering and Technology
Under

Faculty Council of Interdisciplinary Studies Law & Management

Jadavpur University

Submitted By
RISAV DUTTA
Exam Roll No: M4ENR23001
Reg No: 160452 of 2021 - 2022
Roll No: 002130601005
School Of Energy Studies

Under The Guidance Of
Prof. Sudipta De
Supervisor Professor
Department of Mechanical Engineering

Jadavpur University
Kolkata–700032
India
2023

M.Tech Energy Science & Technology
Course affiliated to
Faculty of Engineering & Technology
Under
Faculty Council of Interdisciplinary Studies Law & Management
Jadavpur University
Kolkata, India

CERTIFICATE OF RECOMMENDATION

This is to certify that the thesis entitled "**Optimum sustainable distributed hybrid generation using forecasting and multi-criteria decision making: demonstration for an Indian village**" is a bonafide work carried out by **Mr. Risav Dutta** under our supervision and guidance for partial fulfillment of the requirements for the Post Graduate Degree of Master of Technology in Energy Science and Technology, during the academic session 2021-2023.

THESIS SUPERVISOR
Dr. SUDIPTA DE
Professor
Department of Mechanical Engineering
Jadavpur university
Kolkata–700032

DIRECTOR
Dr. RATAN MANDAL
School of Energy Studies
Jadavpur University
Kolkata–700032

DEAN
Faculty Council of Interdisciplinary Studies,
Law and Management
Jadavpur University
Kolkata–700032

M.Tech Energy Science & Technology
Course affiliated to
Faculty of Engineering & Technology
Under
Faculty Council of Interdisciplinary Studies Law & ManagementJadavpur University
Kolkata, India

CERTIFICATE OF APPROVAL

This foregoing thesis is hereby approved as a credible study of an engineering subject carried out and presented in a manner satisfactory to warranty its acceptance as a prerequisite to the degree for which it has been submitted. It is understood that by this approval the undersigned does not endorse or approve any statement made or opinion expressed or conclusion drawn therein but approves the thesis only for the purpose for which it has been submitted**.**

Committee of --------------------------------------

The final examination for ---------------------------------------

Evaluation of Thesis ---------------------------------------

DECLARATION OF ORIGINALITY AND COMPLIANCE OF ACADEMIC ETHICS

I hereby declare that this thesis contains a literature survey and original research work by the undersigned candidate, as part of his Master of Technology in Energy Science and Technology studies during the academic session 2021-2023.

All information in this document has been obtained and presented in accordance with academic rules and ethical conduct.

I also declare that, as required by these rules and conduct, I have fully cited and referred all materials and results that are not original to this work.

Name	:	**Risav Dutta**
Roll No.	:	**002130601005**
Thesis Title	:	**Optimum sustainable distributed hybrid generation using forecasting and multi-criteria decision making: demonstration for an Indian village**
Signature	:	
Date	:	

ACKNOWLEDGEMENTS

I feel honoured to express my deepest respect, reverence, indebtedness, and heartiest gratitude to my respected supervisor Prof. Sudipta De (Department of Mechanical Engineering, Jadavpur University) for his acute interest in each and every detail of this project, judicious guidance, constant inspiration and help during the entire period of execution of the present project work.

I am also grateful to Dr. Tushar Jash (Professor, School of Energy Studies, Jadavpur University), Dr. Ratan Mandal (Director and Professor, School of Energy Studies), Mr. Sayan Das and Mr. Deepanjan Majumder for their valuable advice and encouragement during the period of the project work.

Finally, I want to thank my parents who have supported me in all ups and downs of my life and have encouraged me all the time without expecting anything in return.

RISAV DUTTA

School of Energy Studies

Jadavpur University

Kolkata–700032

Contents

List of Figures:

List of Table:

Abstract:

The global energy demand is ever increasing. Industrialization, urbanization and growth of population are the primary reasons for the rise in energy demand. About 75% of the total energy in the global power mix is catered by non-renewable energy resources. The transition in the energy sector is towards increasing share of renewable energy. Renewable resources are mostly intermittent. There are Uncertainties in energy demand too as it depends on human activities. A precise forecasting of load demand with selection of combinations of local energy resources to meet that demand will be a feasible solution for distributed energy installations. The objective of this study is to perform an accurate forecasting of the load demand and evaluate its benefit with techno-economic analysis and environmental impact assessment of a hybrid renewable energy system. The load demand of the system was estimated by three different machine learning based forecasting approaches. With the most accurate forecasted result different hybrid energy combinations were verified for an uninterrupted power supply. The best performance for technical, economic and environmental parameters of the integrated hybrid system may not converge at the same combination. To determine the optimum energy system approach is adopted. Multi-criteria decision-making approach is used to determine the optimum solution. The methodology is demonstrated with the data of a remote village in Odisha, India. Forecasting of load demand using fuzzy based method has the least error. Using multi-criteria decision-making approach, it is concluded that the hybrid energy combination with solar photovoltaic - diesel generator–converter - lead acid battery combination is the decided optimum solution for acceptable overall techno-economic and environmental sustainability. This combination of SPV-DG-C-LA has a COE of \$0.100/kWh, NPC of -\$5374 and EE-21.7%, resources- 386120 USD2013, ecosystems- 0.002 species.yr and human health- 1.14 DALY with respect to sustainability.

Keywords: Multi criteria decision making, load forecasting, techno-economic analysis, environmental impact assessment, renewable energy, decentralized hybrid energy system.

Chapter-1

Introduction

1.1 Introduction:

Life without electricity is unimaginable today. About 13% of the global population is yet to get reliable power supply[1]. To provide clean and affordable energy is a sustainable development goal i.e., SDG 7 [2]. On the other hand, global energy demand is ever increasing. The primary cause for the rise in energy demand is the rise in population, urbanization and industrialization. Industrialization and urbanization generally increase, specifically for developing countries like India. Population growth is also inevitable. Considering the present energy scenario, about 75% of the global energy is generated from non-renewable based resources[3]. Burning of fossil fuel generates greenhouse gases which results in global warming. However, under UNFCCC the member countries of COP21 agreed to limit the global rise in temperature below $2^{o}C$ and preferably below $1.5^{o}C$ with respect to the pre-industrial level[4].

About 62% of the total power (about 370 GW) distributed through the national power grid is generated from fossil fuels[5]. As forecasted, by 2040 the national power demand may be three times than that of the present[6]. Extension of the centralized national grid to every corner of the nation is not feasible due to economic and geographic barriers[4].

Renewable energy is generally intermittent, dilute, localized and uncertain due to variations of availability in nature. To accommodate these issues of renewable energy, hybridization is a possible solution[7]. Decentralized hybrid energy system is emerging as a reliable energy solution for remote locations. Following the global trend, India is also adopting decentralized hybrid energy systems for remote locations[4].

The major challenge of a decentralized hybrid energy system is to determine its optimum capacity as well as choosing the most appropriate energy resource combinations[7]. The capacity of a system can be determined on the basis of availability of natural resources vis-à-vis load demand. Estimating the load demand for the future is another major hurdle for decentralized hybrid energy solutions[8]. Load forecasting is the tool to address it. Load forecasting helps for a better energy management through a better power dispatch strategy. It reduces the difference between the future load demand and possible energy generation resulting in improved performance of the energy system[9].

Neither over estimation nor under estimation of load demand is desired as both affects the system performance[10]. Machine learning based forecasting improves the system performance and helps to achieve better overall sustainability. Machine learning based forecasting can be broadly classified into three types, viz., classical, hybrid and fuzzy based. Some of the classical approaches are Artificial Neural Network (ANN)[11], support vector machine (SVM)[12] and Auto-Regression Integrated Moving Average (ARIMA)[13], etc. Hybrid predictive models are Wavelet Analysis (WA), long short-term memory and recurrent neural networks (LSTM+RNN) etc[14]. Adaptive Neuro Fuzzy Inference System (ANFIS) is a fuzzy based approach[15]. Forecasting can also be classified based on time span, say, over a few minutes up to a day (i.e., very short term), days to week (i.e., short term), weeks to month (i.e., medium term) and months to year (i.e., long term)[16].

1.2 Literature Review:

Xiao et al.[17] proposed a dynamic meta-ANN model that records the nano stationary patterns in load dataset. The meta-ANN model is trained using error correction module via gradient descent and reduced error significantly. Jin et al.[18] proposed a hybrid forecasting algorithm using single spectrum analysis and parallel long short term memory (PLSTM) and showed that the accuracy of proposed model is better than PLSTM. Goh et al.[19] proposed a hybrid model with one-dimensional convolution neural network (CNN) and LSTM and showed that the proposed model improve its accuracy than the generic CNN model by 16.33% for single step and 20.33% for 24-step prediction.. Ghenai et al. [15] studied electric load forecasting integrated with smart meters for educational building and showed that the forecasting approach reduces a load uncertainty by minimizing the normalized mean square error (nMSE) (0.4363-4.9576) and normalized mean absolute error (nMAPE) (0.0946 - 0.676). Malik et al.[20] studied the techno-economic and environmental analysis for seven energy combinations for a Himalayan region of India. According to that study, PV-biomass-battery combination is the optimal solution to meet the load at a COE- $0.185/kWh, NPC- $76080 and carbon di-oxide (CO_2) emission-27.8 Mt/year. Khan et. al. [21]designed a stand-alone system for a remote location in North India for capacity of 55.14 kWh/day with a cost of electricity (COE)- $0.152/kWh and a net present cost (NPC)- $34,344. Das and De [22] performed the techno-economic and environmental impact assessment for the possible energy combinations to meet the demand. The study showed that the Solar photovoltaic (PV)- Diesel Generator (DG)-Lithium-ion

(Li-ion) energy combination is the optimal solution to meet the load demand at a COE- \$0.067/kWh, excess electricity (EE)- 14.5% and the total environmental impact assessment is 40.5-82% less as compared to other combinations. Kumar et al. [23] showed that the PV-DG-Zinc 90 Bromide (ZB) battery-converter offers the best techno-economic solution for the considered locations. The combination meets the load at COE- \$0.155/kWh. Das et al. [24] compared five different storage modules and two distinct dispatch strategies combined with the PV-hydro-DG system. According to that analysis PV-hydro-DG-ZB combination meets the required load at a COE \$0.197/kWh under load following (LF) dispatch strategy. Murugaperumal et al. [25] studied the techno-economic feasibility of the hybrid energy combinations using load forecasting methods. The study showed that under the combined dispatch strategy PV-wind-biogen combination could meet the load at NPC Rs.1.21M and COE Rs. 13.71/kWh. Salameh et al.[26] studied the decentralized hybrid energy combinations for Khorfakkan, Sarjah. The study showed that photovoltaic (PV)- diesel generator (DG) combinations met the load demand of 37.75 MWh with a COE- \$0.25/kWh. Kumar and Channi [27] showed that a PV-biomass-battery-converter system meets the load demand of the rural village of Punjab, India at a NPC- \$21087.

1.3 Research gap:

Most of the open literature focus on techno-economically optimal decentralized hybrid energy system. Some compared between dispatch strategies to improve the efficiency of a system. Few studies compared performance of different storage modules integrated in a hybrid energy system. Limited recent studies showed the effect of a stand-alone hybrid energy system on environment. Load uncertainty remains as an obstacle for any stand-alone hybrid energy system. Few studies also reported the accuracy of different forecasting tools. Most of these studies included classical approaches like ANN, ARIMA etc. Few studies demonstrated forecasting using hybrid tools like WA, LSTM-RNN etc. Limited studies performed forecasting using fuzzy based tools. Time span of the forecasting was another factor. Majority of the forecasting were performed for very short term to short term. No significant studies performed both short term and medium-term load forecasting. Integrating time series forecasting coupled with techno-economic analysis and environmental impact assessment of a stand-alone hybrid energy system for overall sustainability assessment is rarely found in published literature.

1.4 Research Objective:

The primary objective of this study is to assess an overall sustainability of a stand-alone hybrid energy system augmented with best fitted load forecasting along with techno-economic analysis and environmental impact assessment. This study compares the accuracy of different forecasting approaches, viz., ANN (classical), LSTM-RNN (hybrid) and ANFIS (fuzzy) through mean absolute percentage error (MAPE) and root mean square error (RMSE). Forecasting performance of these three methods are evaluated for both short and medium terms. The overall sustainability of the proposed standalone hybrid energy system was assessed in terms of techno-economic and environmental parameters. The optimum solution for all the three factors may not converge into a single point. Multi criteria decision making (MCDM) tool is used finally to decide the acceptable solution for overall sustainability. Sensitivity analysis is also performed to determine the robustness of the decided optimum solution. The proposed methodology is novel yet generic as it can be used at any location.

Chapter-2

Materials and Methodology

2.1 Materials and Methodology:

This study estimates the load demand of a decentralized hybrid energy system which in turn reduces the uncertainty of load. As a result, the efficiency of the system is improved. Three different type of machine learning based forecasting tool is adopted. Classical method (ANN), hybrid (LSTM-RNN) and Fuzzy based (ANFIS) are the three different forecasting methods that are adopted to forecast and compare with one another. The study validates the sustainability of the standalone hybrid energy system by techno-economic analysis and environmental impact assessment of the system based on the forecasted data. The different parameters for sustainability of the system may not converge into a single solution. Thus, Technique for Order Preference by Similarity to Ideal Solution (MCDM-TOPSIS) is performed to decide the optimum choice. Further to validate the robustness of the optimum solution, a sensitivity analysis is performed by VIekriterijumsko KOmpromisno Rangiranje (MCDM-VIKOR). The proposed system is demonstrated with an Indian village data.

2.2 Study Area Selection:

The selected village for this study is Uperbeda. The village is situated in Mayurbhanj district of the state of Odisha, India[28]. The latitudinal and longitudinal coordinates of the village is 22.23ºN and 86.52ºE. The livelihood of the village is dependent upon agriculture[29]. The village is yet to receive a reliable power supply[30]. The power supply of this village is currently catered by diesel generators emiting greenhouse gases. Thus, this village is suitable to demonstrate overall sustainability of a decentralized hybrid energy system with load uncertainties[31]. The location of the village is shown in an Indian map in Fig. 1.

(a) (b)

Fig. 1.a: Location in Indian map b: selected village in Odisha district

2.3 Modelling of component modules:

The components of the decentralized hybrid energy system are considered on the basis of availability of natural resources. The schematic diagram of the hybrid energy system is shown in Fig 2.

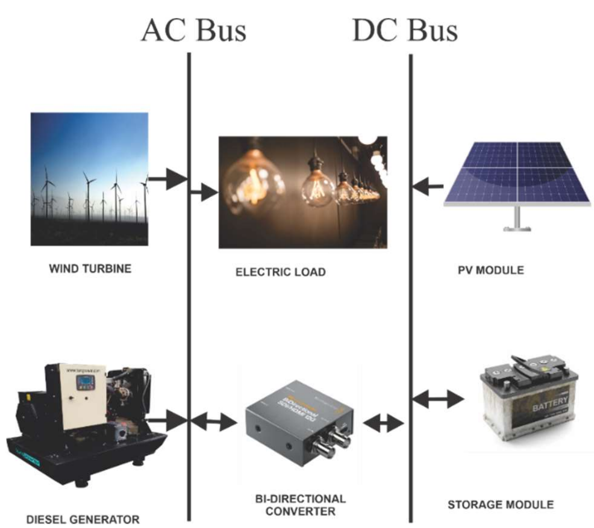

Fig. 2: Schematic arrangement

The components in the proposed module are PV, wind turbine, DG, lead-acid battery and converter. The detailed techno-economic analyses of the component modules are discussed in this section.

2.3.1 PV Module Modelling:

The generated output power of the PV module is estimated using Eq. 1 [32]

$$P_{pv} = Y_{pv,stc} \times f_{pv} \times \frac{I_t}{I_{stc}} \times \left[1 + \delta_t\left(t_{c-}t_{c,stc}\right)\right] \quad (1)$$

Where P_{PV} is the output power of the module in kW, $Y_{PV,\ STC}$ is the rated capacity of the module at standard condition in kW (cell temperature is 25°C, radiation 1kW/m^2), f_{PV} (%) is the derating factor of the module, δ_t is the temperature coefficient of maximum power in %/°C, I_T is the solar radiation at regular condition in kW/m^2 and I_{STC} is the solar radiation at standard condition in 1 kW/m^2, t_c is operating temperature of the solar module at regular condition and $t_{C,\ STC}$ is operating temperature of the solar module at standard condition it is in °C, Tilt angle is set at 28°.

The standard output power of the module varies depending on the cell arrangements. The total number of cells is C. The total power output at the standard condition is estimated using Eq. 2 [33]

$$P_{pv,stc} = (C_s \times C_p) \times P_{max,stc} \quad (2)$$

Where maximum power output of the solar module at standard condition is $P_{max,stc}$ in kW. C_p and C_s are the arrangement of the cells in parallel and series respectively.

A flat plate module was used in this system. The efficiency of the module is 17.49% and the derating factor is 88%. The detailed techno-economic factors are shown in Table 1 [4]. The output power of the module is depending on temperature. The weather data is collected from NASA weather report and shown in Fig. 3[34]. The average solar radiation is 4.78 kWh/m^2/day and the temperature of the location is 24.93°C.

2.3.2 Wind Turbine modelling:

The power generated from the wind turbine is estimated from Eq. 3 [3].

$$P_m = 0.5A \times v^3 \times c_p \times \rho \tag{3}$$

Where P_m is the maximum power generated from the wind turbine in kW, A is the area covered by the blades of the turbine in m^2, c_p is the Benz constant, velocity of the wind is v in m/s [35]. The output wind power of the considered location is dependent on the wind speed of the turbine hub height V_h. It is calculated using Eq. 4[3].

$$V_h(t) = V_{ref}(t) \times \left(\frac{H_h}{H_{ref}}\right)^{\gamma} \tag{4}$$

Where V_{ref} represents the reference wind speed in m/s at any time instance t. H_h and H_{ref} is the hub and the anemometer height in m, γ is known as the Hellman exponent. The value of this exponent depends on several factors such as surface roughness, season, altitude and the temperature of the area etc. [36]. The value of this exponent is one-seventh of the steady wind speed [3].

The 3kW wind turbine is used in this study. The capital and replacement cost of the module are \$1980/kW and \$980/KW respectively. The hub height and the lifetime of the module are 12 m and 20 years. The detailed techno-economic analysis is shown in Table 1 [21]. The wind speed of the location is collected from the NASA weather data [34]. The wind speed data is shown in Fig. 3 and the average wind speed of the area is 3.8 m/s.

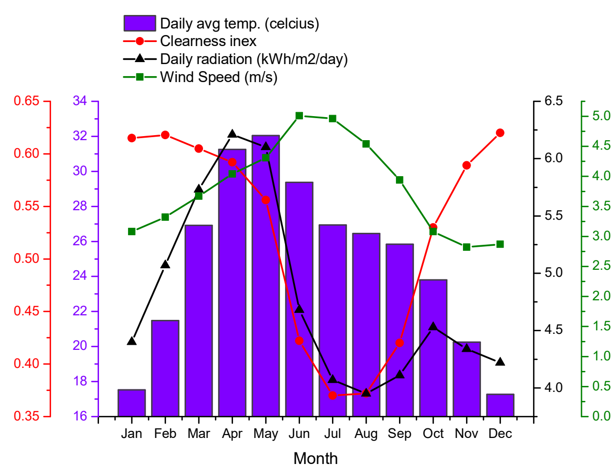

Fig. 3: Natural resources data

2.3.3 Diesel Generator (DG) Modelling:

The power produced from the DG module is estimated using Eq. 5[3].

$$DGC_{G1} = DGC_0 \times Y_{G1} + DGC_1 \times P_{G1} \quad (5)$$

Where DGC_0 and DGC_1 are the coefficient of fuel curve intercept and fuel curve slope in Units/hr/kW, Y_{G1} is the rated capacity of the generator in kW, and P_{G1} is the power output of the generator in kW. The detailed techno-economic specifications are provided in Table 1[3].

2.3.4 Converter:

A bi-directional converter is used in this analysis. The output of the converter is estimated using Eq. 6 [3].

$$Q_{R,out}(t) = J(t) \times \eta_r \quad (6)$$

Where

$$J(t) = Q_{g,\zeta}(t) - Q_{d,\zeta}(t) \quad (7)$$

The conversion of this converter is estimated using Eqs. 8 and 9 [35].

$$Q_{i,out,1} = Q_{DC}(t) \times \eta_i \quad (8)$$

$$Q_{i,out,2} = (Q_{DC}(t) + Q_{batt}(t)) \times \eta_i \quad (9)$$

Where

$$Q_{DC}(t) = \left(L_{ren}(t)\right) \times \Delta t \quad (10)$$

Where the output of the inverter is $Q_{i,out,1}$ which is sufficient to meet the energy requirement $Q_{d,\tau}$ and is fulfilled with energy generated by the system $Q_{g,\tau}$. Q_{DC} is the DC energy available from renewable sources. $Q_{i,out,2}$ is the inverter's output when the energy generated $Q_{g,\tau}$ is not sufficient. The techno-economic details of the module is provided in Table 1 [35].

2.3.5 Storage modelling:

The maximum stored energy in the storage module is calculated using Eqs 11-14[35].

$$S_{bat,cm} = \frac{\min\left(S_{battery,cm,kbm}, S_{battery,cm,mcr}, S_{battery,cm,mcc}\right)}{\eta_{battery,c}} \tag{11}$$

The charging efficiency of the battery is $\eta_{battery,c}$

$$S_{battery,cm,kbm} = \frac{kN_1 e^{-k\Delta t} + Nkc(1-e^{-k\Delta t})}{1-e^{-k\Delta t} + c(k\Delta t - 1 + e^{-k\Delta t})} \tag{12}$$

$$S_{battery,cm,mcr} = \frac{\left(1-e^{-\alpha_c \Delta t}\right)(N_{max} - N)}{\Delta t} \tag{13}$$

$$S_{battery,cm,mcc} = \frac{B_{battery} \times I_{max} \times V_{nom}}{1000} \tag{14}$$

Where N_1 is the available energy in kWh at starting, k is the constant rate of the storage modules in unit per hour, N is the available energy in the module in first time step (kWh), α_c is the maximum charge rate of the storage module (A/Ah), N_{max} is the maximum storage capacity of the module in kWh, Δt is the time span in h, c is the capacity ratio of the module, $B_{battery}$ is the total battery , I_{max} is the maximum amount of current in A and the nominal voltage is V_{nom} in V. The Lead-acid battery (LA) is considered in this analysis. The detailed techno-economic specifications are provided in Table 1 [35].

Table 1: Techno-economic specifications of the components

EQUIPMET	PARAMETER	SPECIFICATION
PV module	TYPE	flat plate
	Maker	Canadian Solar
	Derating factor	88%
	Initial cost ($/kW)	1667
	Cost of replacement ($/kW)	1667
	O&M cost ($/kW/year)	19.38
	Lifetime (years)	25
	Operating temperature (◦C)	45
	Efficiency (%)	17.49
	Capacity (kW)	3
	Temperature coefficient	-0.41
	Rated capacity (kW)	0.34
Wind turbine module	Maker	AWS
	Initial cost ($/kW)	1980
	Cost of replacement ($/kW)	980
	O&M cost ($/kW/year)	25
	Lifetime (years)	20
	Hub height (m)	12
	Rated capacity (kW)	3.3
	Rotor diameter (m)	4.65
Diesel generator module	Initial cost ($/kW)	250
	Cost of replacement ($/kW)	160
	O&M cost ($/kW/h)	0.03
	Fuel cost	1.2
	Type of fuel	Diesel
	Lifetime (h)	15000
	Minimum Load ratio	25
Converter	Initial cost ($/kW)	700
	Cost of replacement ($/kW)	10
	O&M cost ($/kW/h)	500
	Efficiency (%)	95
	Relative capacity (%)	100
	Lifetime (years)	15
Storage Module	Type	Lead acid (LA) battery
	Initial cost ($/kW)	240
	Replacement cost ($/kW)	190
	O&M cost ($/kW/year)	2
	throughput(kWh)	10,930
	string size	1
	initial state of charge (%)	100
	minimum state of charge (%)	20

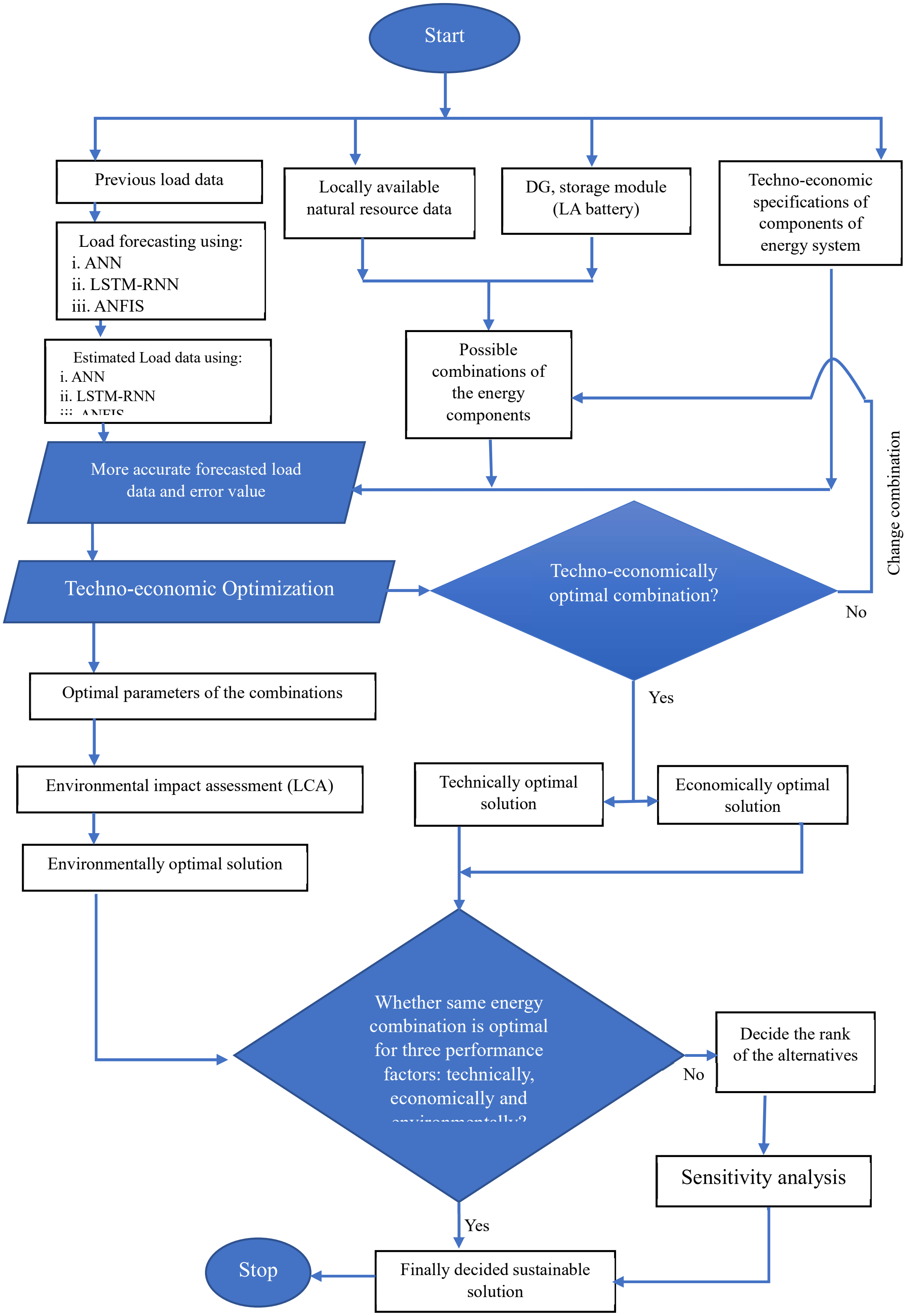

Fig. 4: Methodology flowchart

2.4 Methodology:

The methodology of the entire study is demonstrated with the help of an integrated flowchart in Fig 4.

2.4.1 Forecasting Approach:

Three different forecasting approaches are used to perform the load forecasting of the decentralized hybrid energy system. The different forecasting approaches are ANN, LSTM+RNN, and ANFIS.

2.4.2 Artificial Neural Network (ANN) methods:

ANN model replicates the human brain in terms of neural structure [7]. The detailed construction and working principle of ANN is shown in Fig.5. [37]. According to the ANN structure and the working principle the model has to be trained through iteration. The method predicts in terms of time series and sequential prediction [38]. The accuracy of the predicted values is estimated using the testing set. The output data of the ANN model are calculated by using Eqs. 15-16 [38].

$$y_i = b_{j+\sum_{i=1}^{n} w_{i,j} a_i} \tag{15}$$

$$p_j = f(y_j) \tag{16}$$

Where the input values are *a*, the output value is *p,* the weighted coefficient is *w, n* is the number of neurons in the layer and it has the same number of input values. *J* is a subsequent neuron in the layer. The inputs '*a's* are integrated with the weighted coefficient *w* and added to the bias b_j, f is the activation function and p_j is the output for the particular input.

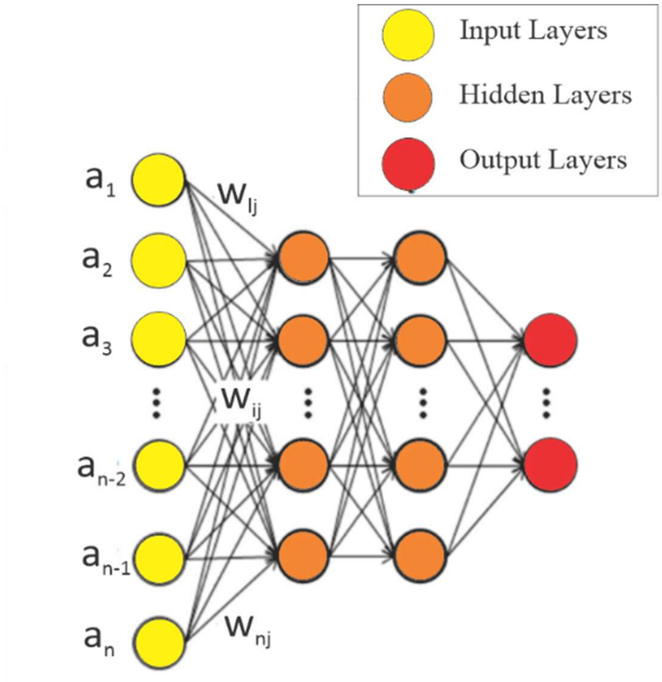

(a)

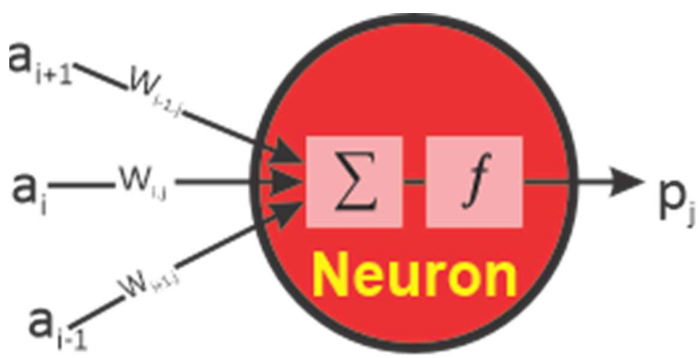

f: activation function
$\sum$: Total sum of weighted inputs and bias

(b)

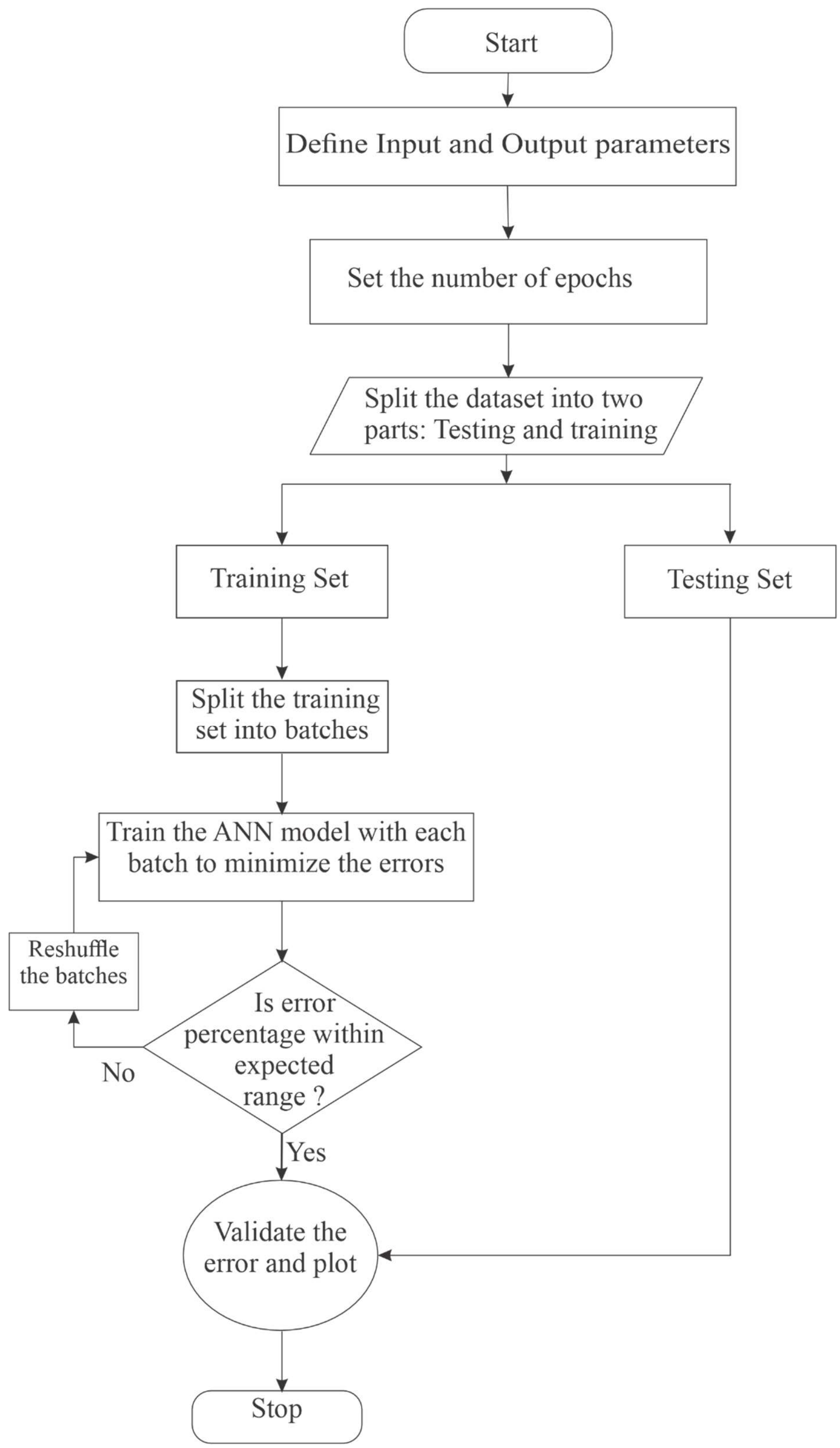

(c)

Fig. 5 a: Structure of ANN b: Internal structure of neuron c: Flowchart of ANN

2.4.3 Load prediction using LSTM and Recurrent Neural Network (RNN):

The LSTM+RNN approach is different from the generic feed-forward neural network. The previous data obtained through this method is transferred to the current time-frame. LSTM works on the principle of back propagation. At times RNN faces a problem known as the vanishing gradient [39]. The LSTM unit comprises a cell and three gates which are controlled by the sigmoid activation function [40]. RNN structure is shown in Fig. 6a [41] and Fig. 6b represents the LSTM structure [42]. Figure 6c. shows the working principle of the method [43]. The equations associated with the LSTM+RNN method are described in Eqs. 17-18 [42].

LSTM+RNN forecasting method:

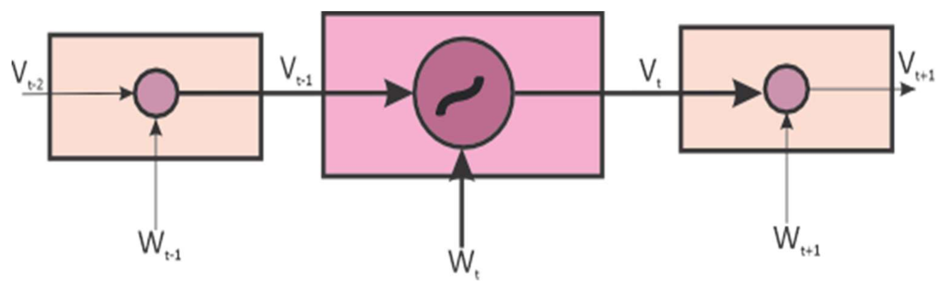

(a)

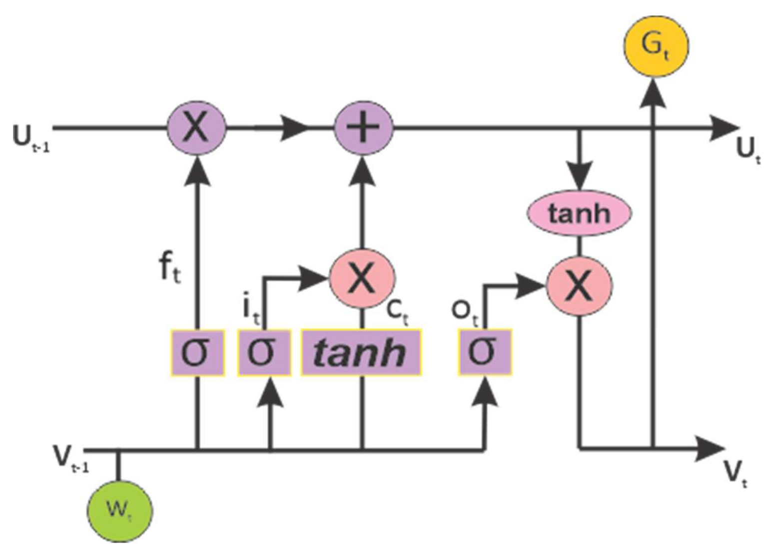

(b)

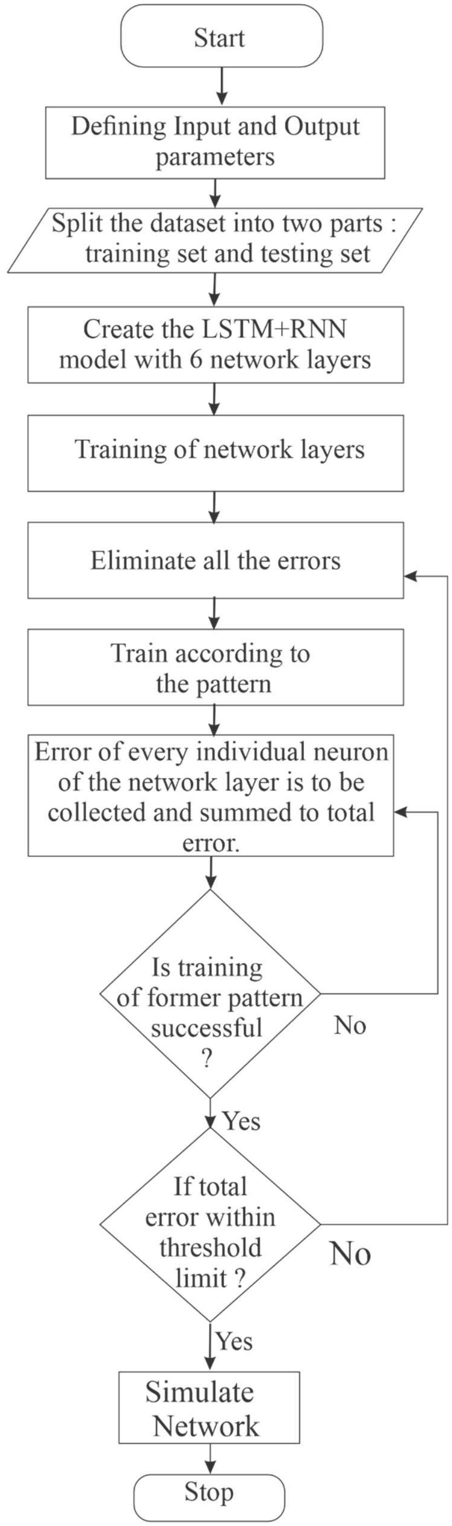

(c)

Fig. 6: a: Structure of RNN b: Structure of LSTM c: Flowchart of LSTM+RNN

$$u_t = f_t.u_{t-1} + i_t.c_t \tag{17}$$

Where c_t is

$$c_t = \tanh\left(k_m.[v_{t-1}, y_t] + j_m\right) \tag{18}$$

Where u_t is the memory cell, t is the present and t-1 is the previous time step, k_m is the memory cell's weight matrix and the hidden state is v, y_t is the input at time t and j_m is the bias for memory cell, i_t is the input gate, f_t is the forget gate, o_t is the output and h_t is the hidden cell state. These are calculated using Eqs. 19-22 [42].

$$i_t = \sigma(k_i[h_{t-1}, y_t] + j_{i)} \tag{19}$$

$$f_t = \sigma(k_f[h_{t-1}, y_t] + j_{f)} \tag{20}$$

$$o_t = \sigma(k_o[h_{t-1}, y_t] + j_{o)} \tag{21}$$

$$h_t = o_t * \tanh(u_t) \tag{22}$$

2.4.4 Adaptive neuro fuzzy inference system (ANFIS):

The fuzzy logic was introduced by Lotfi Zadeh in 1965 to achieve a definite conclusion from a set of uncertain information [44]. Roger proposed the ANFIS method under fuzzy forecasting approach to predict the time series model of nonlinear functions and components [45]. This method helps with quick learning, expresses the nonlinear structure of a process, and has good adaptability.

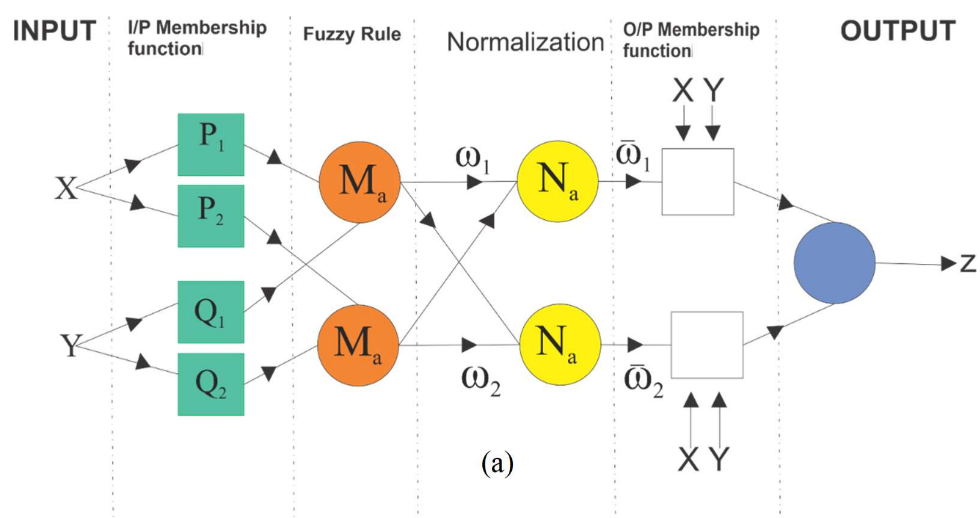

(a)

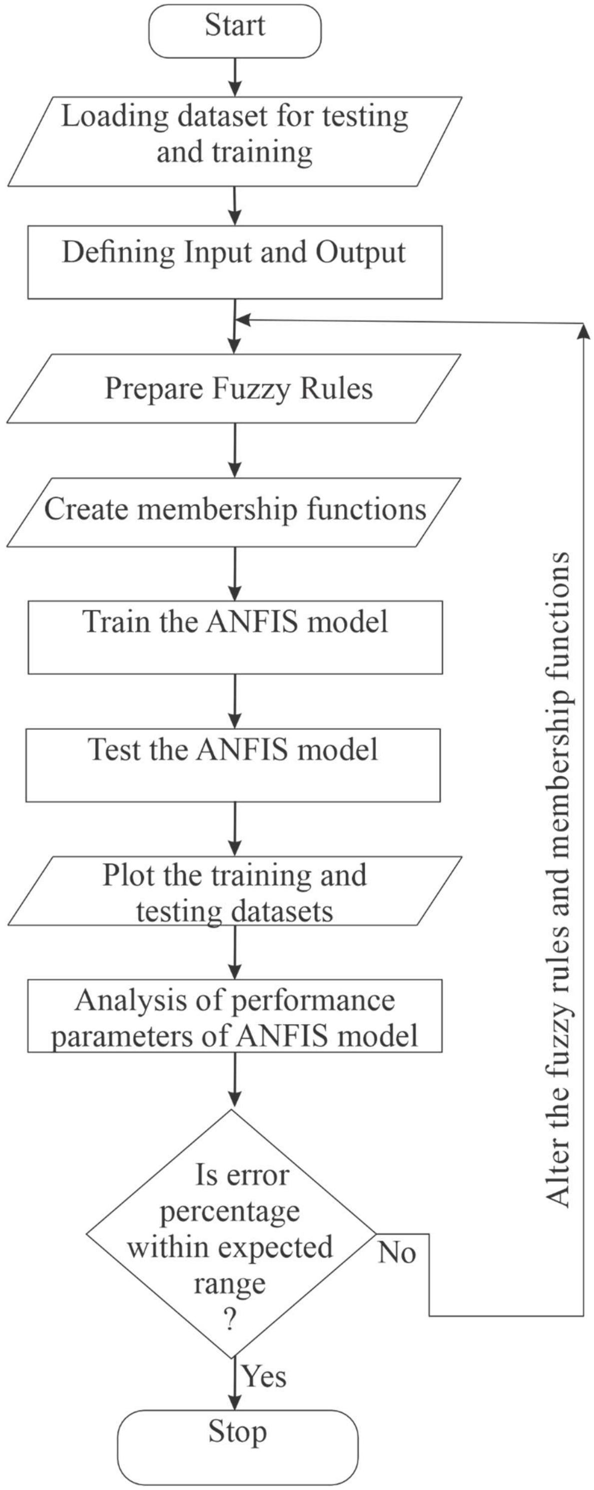

(b)

Fig. 7 a: Structure of ANFIS b: Flowchart of ANFIS

According to the working principle shown in Fig. 7a and 7b the ANFIS works in five segments. The first segment is the input membership function which carries out the fuzzification process with the two inputs p and q. The output from the first segment is the membership form of the inputs of the same segment. The second segment is the rule, here the output expresses the fuzzy strength of each rule. Each node of this segment acts as a multiplier thus it is labelled with M_a. The next segment is the third segment here the fuzzy strength is normalized. The normalizing factor is obtained from the total of the weight function**.** Since this layer is acting as the normalizing segment thus all the nodes of this segment are labelled with N_a. ω_i is the fuzzy strength used to normalize the output. Output membership function with adaptive nodes is the fourth segment, and its output are represented by $\omega_i z_i$ represents the output membership function. The outputs, z_i (i = 1, 2), within the fuzzy region specified by the fuzzy rules and it is given Eq. [23, 24].

$$z_{i=p_i x+q_i y+r_i} \tag{23}$$

Where p_i, q_i, and r_i are the parameters of the membership functions determined during the training process

To optimize the parameters of the membership functions in the ANFIS training process, a hybrid learning technique using the gradient descent approach and the least-squares estimate is used. The last layer (layer 5) represents the overall output. This layer contains only one fixed node. The total incoming signals of this node is calculated by using Eq. 24.

$$z_i = \sum_{i=1}^{2} \overline{\omega}_i z_i \tag{24}$$

The MAPE and RMSE are calculated for the different forecasting methods by using Eqs. 25 and 26.

$$M.A.P.E. = \frac{1}{S}\sum_{i=1}^{S}\left|\frac{y_{forecast}-y_{target}}{y_{forecast}}\right|.100\% \quad (25)$$

$$R.M.S.E. = \sqrt{\frac{1}{S}\sum_{i=1}^{S}(y_{forecast}-y_{target})^2} \quad (26)$$

2.5 Hybrid Optimization of Multiple Electric Renewable Simulation:

The HOMER® software is developed by the National Renewable Energy Laboratory (NREL), USA to perform the techno-economic performance analysis of energy systems. It performs an analysis and ranks different energy combinations according to desired parameters. It analyzes different combinations and ranks the model according to the economic performance factors. The working principle of HOMER® is shown in Fig. 8

The analysis is performed based on different dispatch strategies. According to this study, the load following (LF) dispatch strategy is the most acceptable one. In this study the techno-economic analysis is performed under this dispatch strategy. The working principle of the method is shown in Fig. 9

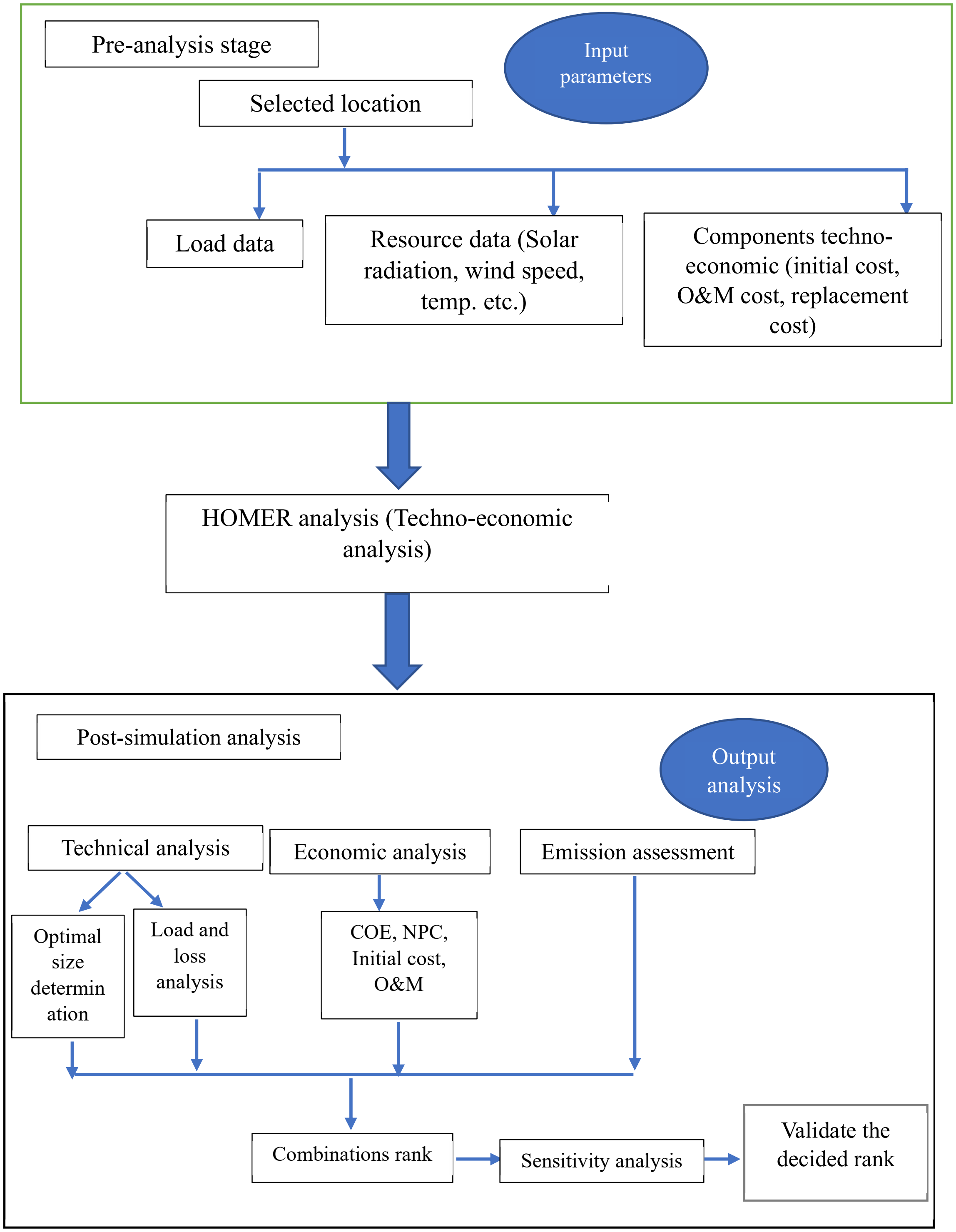

Fig. 8 Working Principle of HOMER

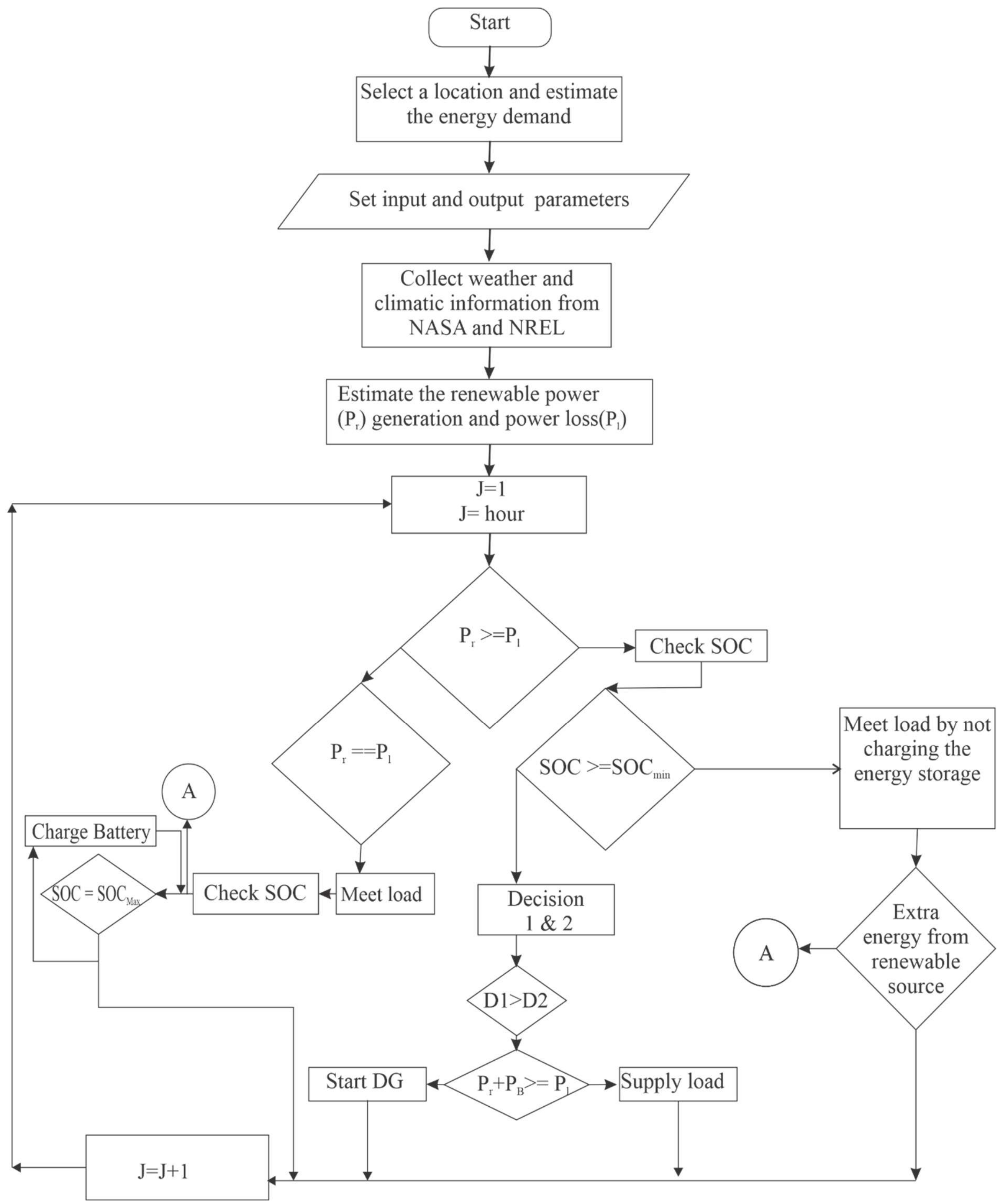

Fig. 9 Working principle of load follow dispatch strategy

2.6 LCA approach:

The impacts of the proposed decentralized hybrid energy system on nature, ecosystem, and environment are analyzed using the LCA method [46]. The LCA analysis is performed in SimaPro® 9 which follows the guideline of ISO 14040/44 [47]. The analysis is accumulated in four steps, i.e., Goal and scope, data inventory, impact assessment and interpretation [46]. The working principle of the LCA method is shown in Fig. 10.

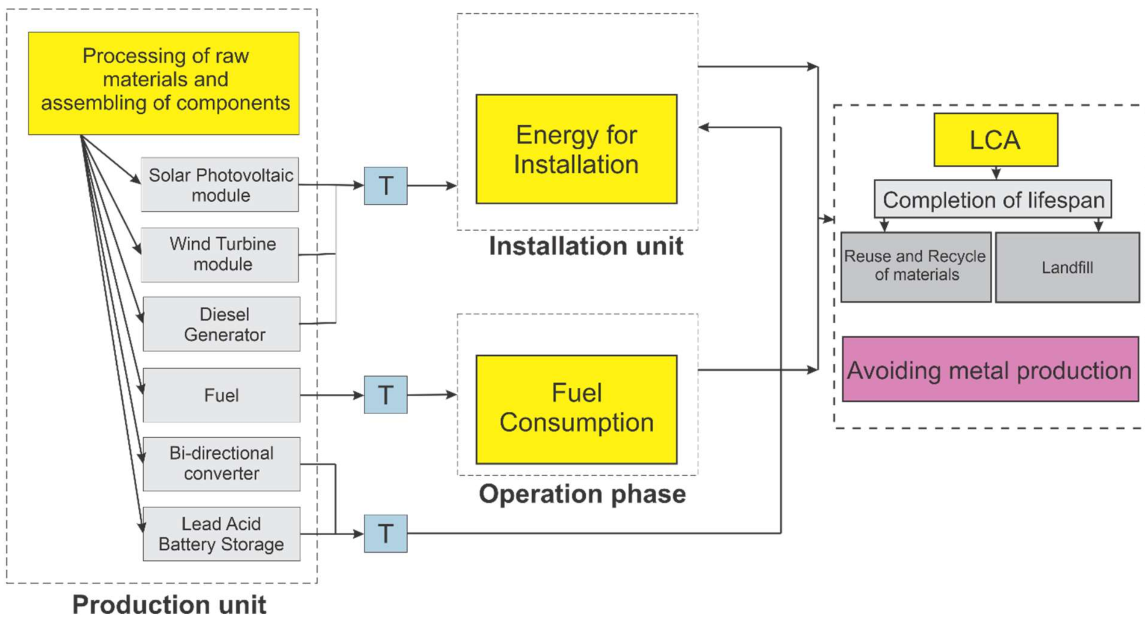

Fig. 10 LCA approach

2.6.1 Goal and Scope:

The documentation of the process is done in this Goal and Scope step [35]. In this study the goal of the LCA is to analyze the environmental impact of the decentralized hybrid energy system during its full lifespan. The scope of this study is 'from cradle to grave' [48]. Figure 10 shows the boundaries of the process. This LCA process accumulates the raw materials, assembling, transportation, installation, functioning of the system followed by the disposal at the end of its life expectancy. In this study, generation of 1kWh electricity is referred to as one functional unit [3]

2.6.2 Data Inventory:

The Eco-invent 3.1® database is used in this study. Considering this process, the raw material data of the considered modules such as PV module [48], wind module [49], DG, converter and LA battery are collected from different sources [3]. Data of the raw material is collected from open literature and manufacturer's data. The data is shown in Table 2- 6 [3]. The Eco-invent 3.1® database is used for assembling and installing the components and also to calculate the transportation of the components[50]. Total energy required for transportation is the sum of energies required for transporting individual equipment of a system and it is shown in Eq. 27 [50].

$$T_k = H_{t_k}^* \times d_k^* \times s_k^* \tag{27}$$

Where H_{tk}^* is the shipment weight, d_k^* is the distance travelled and the intensity is s_k^*. The total transportation is shown in Table 7.

Table 2 : Data inventory of solar module [45]

Lifecycle Stages		Values
Installation material	Diesel to mount PV module in floor (GJ)	0.00174
	Electricity to mount PV in roof (kJ) (low voltage)	160
	Electricity to mount PV in floor (KJ) (low voltage)	30
Raw material	Multi silicon waver (ft^2)	10.7639
	Electrical parts (pieces)	0.04
	Mounting system required for PV module (ft^2)	10.44099

Table 3: Data inventory of wind turbine [46]

Lifecycle Stages		Values
Fixed part's raw materials	Low alloyed steel (kg)	13100
	Normal Concrete (m^3)	80.8
	Reinforced Steel (g)	9100000
Raw materials (moving parts)	Glass fibre (g)	1160000
	Alloyed wrought aluminium (g)	260000
	Copper (kg)	910
	Unsaturated polyester resin (kg)	60
	Steel- Hot rolled (g)	4680000
Installation details	Explosive tovex (g)	20600
	Diesel (GJ)	0.1044

Table 4 : Data inventory of convertor [3]

Lifecycle stages		Values
Components	Cast aluminium alloy (kg)	1.4
	Copper (kg)	5.5
	Capacitor (kg)	0.6
	Corrugated board box (kg)	2.4
	Glass diode (kg)	0.05
	Polyethylene fleece (g)	60
	Clamp (g)	240
	Ring core of inductor (kg)	0.35
	Metal (factory)	8.9E-9
	Logic type circuit (g)	30
	Slab of polystyrene (g)	300
	Polyvinyl chloride (g)	1.11
	Aluminium section bar, extrusion (kg)	1.4
	Printed wiring box (g)	225
	Steel sheet (kg)	9.8
	Resistor (g)	5
	Low alloyed steel, Hot rolled (kg)	9.8
	Wired transistor (kg)	0.04
	SAN copolymer (g)	10
	Copper for wire drawing (kg)	5.51

Table 5 :Data inventory of DG [3]

Lifecycle stages		Value
Components in kg	Alloy of aluminium	32.8
	Copper	40.1
	Cast iron	141
	Lead (Pb)	0.7
	Cast allow of aluminium	31
	Molybdenum	1.7
	Liquid epoxy Rasin	3.3
	High-coal 74.5% ferro manganese,	6.1
	Nickel (Ni)	2.7
	White board printed	1.5
	Pig iron	179.3
	Chromium steel (18/8)	2.5
	Zinc (Zn)	0.4
	Tin (Sn)	0.5
	Titanium	0.4
	Steel, low alloyed	498.3
	Silicon carbide	146.7
	Low alloyed steel, hot rolled	121.9
Installation	Heat in GJ	65.3
	Electricity in GJ	19.6

Table 6: Data Inventory of LA battery [3]

Life cycle stage		Value
Components	Anode (kg)	0.312
	Cathode (g)	300
	Electrolyte (g)	140
	Separator (g)	40
	Electronic (g)	90
	Casing (g)	150
Installation	Electricity (MJ)	0.7

Table 7: Transport data [47]

Mode of transport	Route	Distance
Railway, freight train (IN)	Factory to the urban store room	1000 km
Road, freight lorry, 16–32 metric ton. Euro5	Urban store room to regional store room	600 km
Short distance road, freight lorry,3.5–7.5 metric ton. Euro4	Regional store room to installation destination	150

2.6.3 Impact assessment:

To perform the LCA and assess the impact, the ReCiPe 2016 V1.1 process of SimaPro® is used in this study [51]. According to the guidelines of ISO 14040/44, LCA is to evaluate and get through the potential of environmental impacts of the module. The environmental impact is done through the mid-term and the end-term analyses. In mid-term analysis the impact is divided into 18 different characteristics. In the endpoint analysis these 18 characteristics are summarized in 3 different characteristics through Eco-indicator 99® (EE), i.e., human health, ecosystem impact and resource scarcity. The details of these two steps are discussed in Table 8 and 9. In this study the endpoint analysis is considered to determine the environmental impact of the components.

Table 8: Midpoint characteristics [48]

Environmental characteristics	Description	Unit
Climatic change	1000 years are required to change the egalitarian perspective of environment. CO2 is major cause.	y/kg CO_2 to air
Stratospheric ozone depletion	Ozone depletion in stratosphere leading to ozone hole formation caused mainly due to CFC.	y/kg CFC11 to air
Ionizing Radiation	This is emitted from radionuclides. Energy generation from fossil fuels is a process of its emission.	y/kBq Co-60 to air
Fine particle formation	Emission of $PM_{2.5}$ particles along with NO_x and SO_x causing hazard to life.	y/kg $PM_{2.5}$ to air
Photochemical ozone formation	Ozone formation by photochemical reaction which is used to evaluate characterization factor for each volatile organic compound.	y/kg NO_X to air
Terrestrial acidification	Soil sensitivity in accordance to hydrogen concentration.	y/kg SO_2 eq
Freshwater eutrophication	Addition of excess unnecessary nutrients to the water.	Species.y/kg to air
Toxicity	This factor solely indicates carcinogenic and non-carcinogenic effect along with extensive modelling of dissociating organics.	y/kg 1,4-DCB to air
Land use	Use of land causing damage to the environment and ecosystem.	m2a crop eq
Mineral resource scarcity	The shortage of minerals is supported by recycling of minerals. Though recycling is not sufficient at time.	kg Cu eq
Fossil resource scarcity	The shortage of fossil fuel for future use, estimated by modelling.	kg oil eq
Water usage	Water usage is indicated at the end-point level. It is indicated with ratio.	m3

Table 9: Endpoint characteristics [48]

Protection area	Endpoint	Abbreviations	Unit
Human health	It indicates the hazard caused to the human health.	HH	year
Natural environment	It indexes indicate the damage to the nature and ecosystem.	ED	Species*y
Resource scarcity	It indicates the depletion to the natural resources.	RA	Dollar

2.7 Multi-criteria decision-making approach:

As the optimum alternatives may not converge into the same point, the finally acceptable solution needs to be decided using a MCDM approach. MCDM is used to decide the rank of different alternatives and determine the best feasible solution.

2.7.1 Technique for Order of Preference by Similarity to Ideal Solution:

TOPSIS is an extensively used MCDM approach. It works on the principle that it should be closest to the best solution and farthest from the worst solution. The weights of the criteria are decided in a discrete way. The steps to perform TOPSIS-MCDM are:

Step 1: Attributes to be selected.

Step 2: Decision matrix named as X is formed using p alternatives and q criteria, scores are allotted for each attribute and alternative. The matrix is formed using these scores.

$$X = \begin{bmatrix} a_{11} & a_{12} & a_{13} \\ a_{21} & a_{22} & a_{23} \\ \vdots & \vdots & \vdots \\ a_{q1} & a_{q2} & a_{q3} \end{bmatrix}$$

(28)

Step 3: Using the eq.() the matrix Z is obtained.

$$z_{ij} = \frac{e_{ij}}{\sqrt{\sum_{i=1}^{p} e_{ij}^{2}}} \quad (29)$$

Where, z_{ij} is a element of normalized matrix Z and e_{ij} is a elements of the matrix in the i^{th} column and j^{th} row. i= 1,2,3,4,…..p and j= 1,2,3,4…….q.

Step 4: Weighted normalized decision matrix is to be calculated.

$$l_{ij} = w_{ij} \times w_i \quad (30)$$

Where, l_{ij} is an element of the weighted normalized matrix.

Step 5: Estimation of the best and worst ideal solution is to be made. In case of beneficial criteria highest value is taken into count and for non-beneficial criteria lowest value is looked for.

$$K^{+} = \left(l_1^{+}, \dots \dots l_j^{+}, \dots \dots l_q^{+}\right) = \left\{\left(max_{jl_{ij}} \middle| j = 1, \dots., p\right) i = 1, \dots., q\right\} \quad (31)$$

$$K^{-} = \left(l_1^{-}, \dots \dots l_j^{-}, \dots \dots l_q^{-}\right) = \left\{\left(max_{jl_{ij}} \middle| j = 1, \dots., p\right) i = 1, \dots., q\right\} \quad (32)$$

Step 6: Calculation of the Euclidian distance from the best and worst ideal value.

$$S_i^{+} = \sqrt{\sum_{j=1}^{n} \left(l_j^{+} - l_{ij}\right)^2} \quad (33)$$

$$S_i^{-} = \sqrt{\sum_{j=1}^{n} \left(l_j^{-} - l_{ij}\right)^2} \quad (34)$$

Step 7: Considering this the performance score (g_i) is calculated and corresponding rank of the model is given.

$$g_i = \frac{S_i^{-}}{S_i^{-} + S_i^{+}} \quad (35)$$

2.7.2 Sensitivity analysis:

The robustness and the consistency of the obtained solution is evaluated through sensitivity analysis. For this analysis another MCDM approach, i.e., the VIKOR-MCDM method is considered [52]. The working principle of this method is discussed in Fig. 11[53].

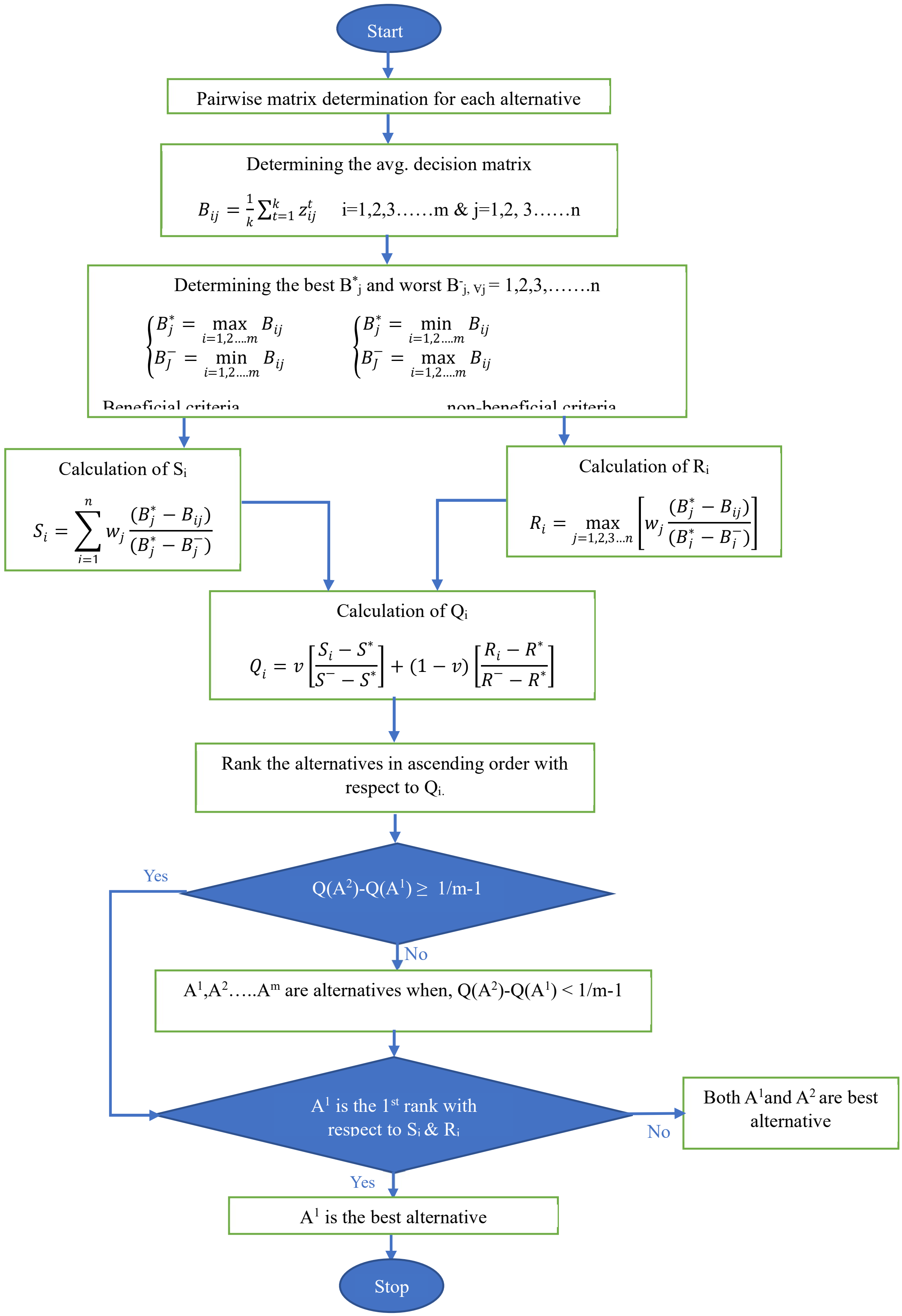

Fig. 11 VIKOR-MCDM working principle

2.8 Load Estimation:

The load data is estimated using the mathematical modelling process [4]. The estimated load data is shown in Fig. 12. The sample load is estimated for a few households. The total load is considered as 11.44 kWh/day. The average load is 0.48 kW and the peak load is 1.13 kW with a load factor 0.42.

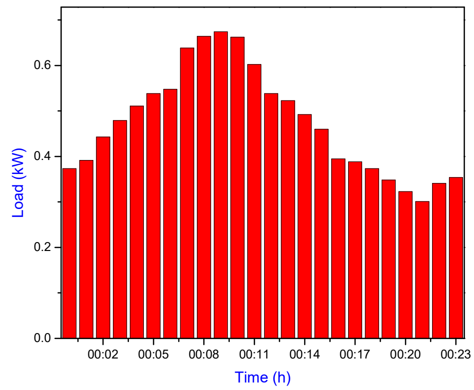

Fig. 12 Load curve

2.9 Objective function and Design Parameters:

The details of the objective function and the design parameters are discussed below:

2.9.1 Annualized cost:

The annualized cost (C_A) of a system is the total sum of the initial cost (C_i), operation and maintenance cost ($C_{o\&m}$) and the cost of replacement (C_R) for the overall year Y. For fuel-based equipment the cost of fuel consumed in a year (C_{fy}) is also considered for the annualized cost. The units are in US$. Equation 36 shows the annualized cost [35].

$$C_A = C_{o\&m} + C_i + C_R + C_{fy} \tag{36}$$

2.9.2 Net present cost:

Net present cost ($/Year) is the present cost of an equipment or a system considering depreciation and other parameters and it is estimated using Eq. 37.

$$C_{NPC} = \frac{C_A}{CRF(i,t)} \tag{37}$$

Where C_A is considered to be the annualized cost of the project ($), CRF is the Capital recovery factor, the project lifetime is Y years and the rate of interest per annum is i in % and it is calculated using Eq. 38 [35].

$$i = \frac{i_n - f}{1+f} \tag{38}$$

Where f is the inflation rate and i_n is the nominal rate of interest (%).

2.9.3 Cost of electricity:

Cost of electricity (COE-$/kWh) is the average cost of one unit of electricity during the lifetime of the project. The system is considered to be a renewable hybrid model containing both renewable source and diesel generator. COE is estimated using Eq. 39 [35].

$$COE = \frac{C_A}{E_A} \tag{39}$$

Where E_A is the electricity consumed in a year (kWh/year) and C_A is the annualized cost of the project in $. In this study, the penalty cost for emission is considered as $10/ton.

2.9.4 Excess electricity:

Intermittent renewable resources may produce more power than required demand at any instant and also if the state of charge (SOC) of the storage module is full then this surplus electricity is known as excess electricity (EE). It may be dumped into the atmosphere as heat through suitable ballasts. It is estimated using Eq. 40 [35].

$$EE(\%) = \frac{E_{excess}}{E_{Gen}} \times 100 \tag{40}$$

Where E_{Gen} is the total amount of energy produced during a particular year and E_{excess} is the excess amount of energy produced per year in (kWh/year).

2.9.5 Renewable Fraction:

Renewable fraction (RF) is the fraction of energy generated from renewable sources compared to the net amount of energy produced by a hybrid energy system. It is estimated using Eq. 41.

$$R_f = \frac{E_r}{E_n} \times 100 \tag{41}$$

Where R_f is the renewable fraction of the project, E_r and E_n are the energy derived from the renewable sources of the project and total amount of energy generated from the project respectively.

2.9.6 Unmet Load:

The electrical load of the decentralized grid which is not met through energy generators is known as the unmet load (UL)-% and it is expressed in Eq. 42.

$$UL = \frac{L_{NF}}{L_{Tot}} \times 100 \quad (42)$$

Where L_{NF} is the load that is not met through energy generators and L_{Tot} is the total required load during the year.

2.9.6 Objective function:

All the input parameters are expressed into a single objective function to perform the simultaneous optimization. The weights of the factors are decided according to their priority.

The objective function of this analysis is shown in Eq. 43.

$$f_{obj} = W_c \times COE + W_N \times NPC + W_E \times EE + W_{EIA} \times EIA + W_{UL} \times UL + W_{GHG} \times GHG \quad (43)$$

Where Wc, WN, WE, WEIA, WUL, WGHG are the weighting factors for COE, NPC, EE, environmental impact, UL and greenhouse gas respectively. The normalization factors for the input parameters are considered to convert the values within an order of 10. The weight factors are decided according to the priority and from the previous literature [52]. Higher the priority of the optimization, the weight factors value is also high. The economic weight is 0.5, environmental weight is 0.3 and the other two weights are 0.1 respectively.

Chapter-3

Results and Discussion

3.1 Result and Discussion:

The study performs load forecasting using three different machine learning-based approaches and determines the most accurate forecasting approach in terms of MAPE and RMSE. The error in the forecasted load demand and the load values are used to process the optimization of the techno-economic parameters. Load forecasting helps to reduce the uncertainty of future load demand. As a result, the techno-economic performance of the standalone hybrid energy system is improved. The impact of different energy combinations on the environment is assessed by performing a full LCA. A combined load demand forecasting, techno-economic analysis and environmental impact assessment are performed to determine an efficient and sustainable decentralized hybrid energy system combination. ANN, LSTM+RNN, and ANFIS are the forecasting approaches adopted to estimate the load demand of the decentralized hybrid energy system. Using the forecasting approaches extrapolation of load demand is performed. MCDM is finally performed by allotting similar weights to different parameters as the optimum combination for different parameters may not converge. Finally, to verify the robustness sensitivity analysis is performed.

3.2 Forecasting analysis:

ANN, LSTM+RNN & ANFIS are the three forecasting approaches adopted for forecasting the load demand of the decentralized hybrid energy system. The forecasting was performed for the short-term and medium-term. The regression analysis and forecasting results are shown in Fig**. :**13-15.

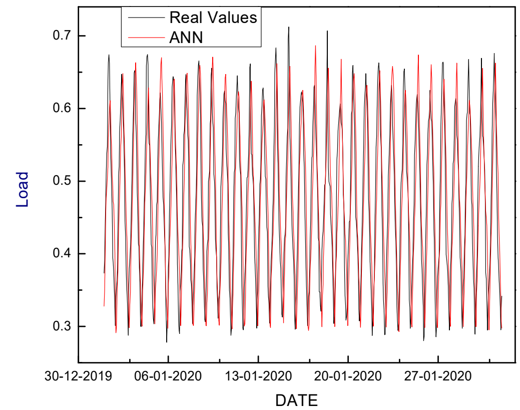

(a)

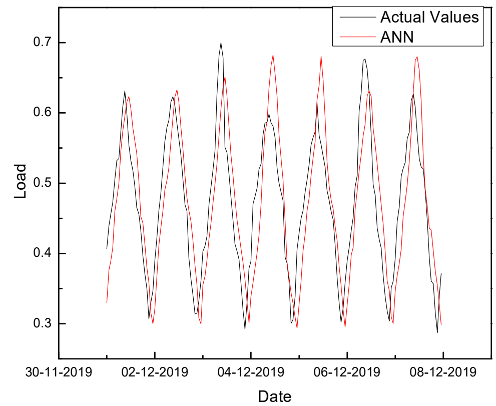

(b)

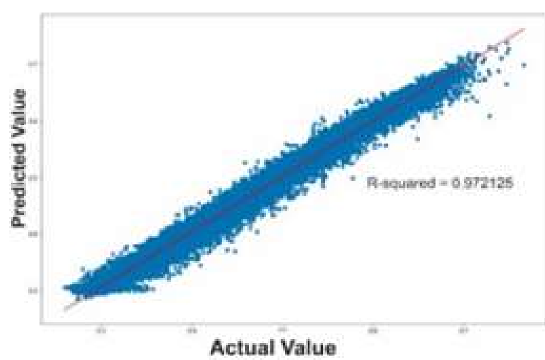

(c)

Fig. 13 a: ANN forecasting Actual vs predicted (monthly) b: weekly c: regression model

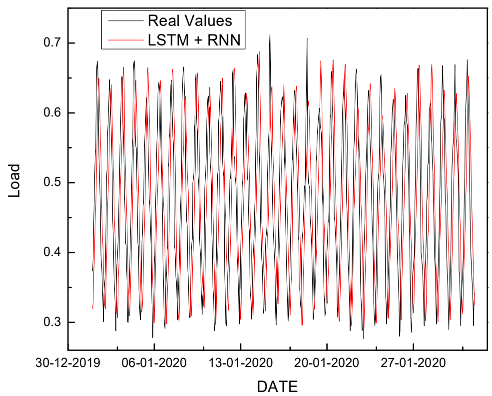

(a)

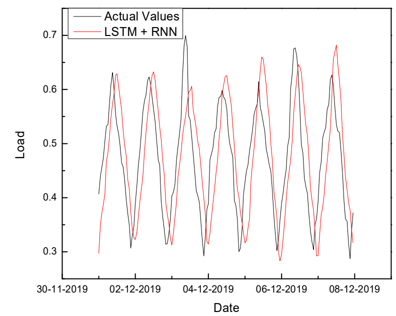

(b)

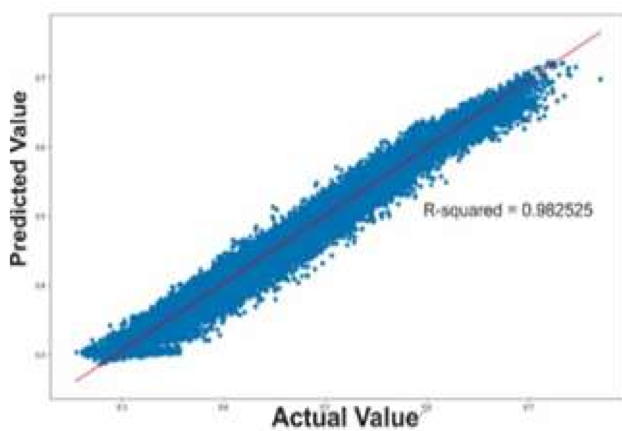

(c)

Fig. 14 a: LSTM+RNN Actual vs predicted (monthly) b: Weekly c: Regression model

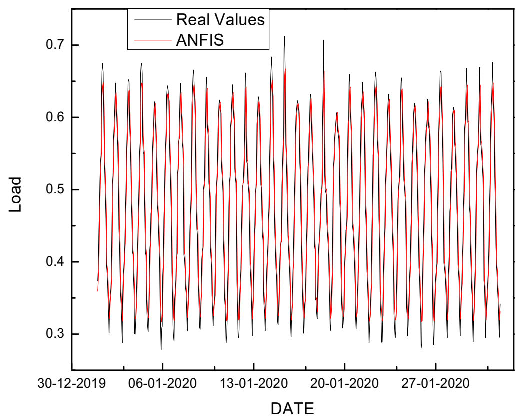

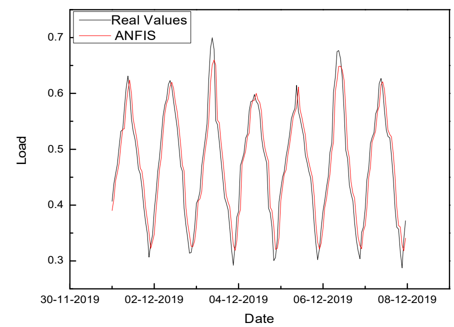

(a) (b)

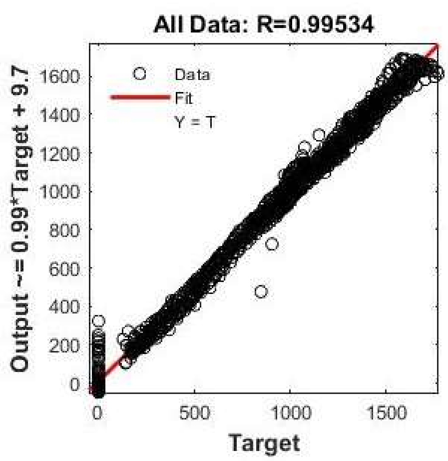

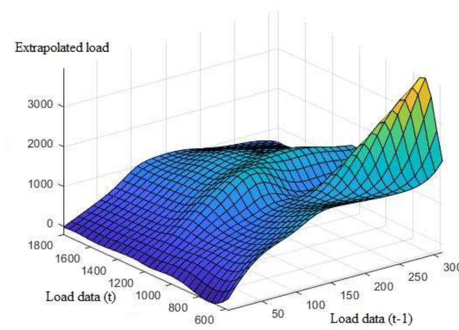

(c) (d)

Fig. 15 a: ANFIS forecasting Actual vs predicted (monthly) b: weekly c: regression model d: Surface determination

By evaluating the regression plot obtained from the different forecasting approaches it can be seen that the regression value for the ANFIS method is best at 0.99534 whereas the regression values for ANN and LSTM+RNN are 0.972125 and 0.982525 respectively. This shows that the forecasted result from the ANFIS method is more exact compared to those by the ANN & LSTM+RNN. From weekly forecasting or medium-term forecasting, it is clear that the load demand forecasted using the ANFIS method is more accurate as compared to others. A surface plot is obtained from the ANFIS forecasting as two datasets including the present hour and previous hour are fed as input and single output is obtained.

ANFIS i.e., a fuzzy-based tool shows the least error value among all. Table 10 shows the MAPE and RMSE values of different forecasting approaches.

Table 10: Details of forecasting

	ANN		**LSTM + RNN**		**ANFIS**	
	TEST	**TRAIN**	**TEST**	**TRAIN**	**TEST**	**TRAIN**
RMSE	0.61	0.61	0.017	0.0171	0.016	0.0166
MAPE (%)	4.274	4.274	4.1344	4.1344	4.0024	4.0024
Regression Value	0.9721		0.9825		0.994	0.995
No. of epochs	200		200		200	
No. of hidden layers	3		6		NA	

The MAPE value for the ANFIS method is 4.0024, which is the least. The MAPE for the ANN method is 4.274 which is 6.78% more than that of ANFIS. The MAPE of LSTM+RNN is 4.1344 which is 3.26% more than that of ANFIS. The RMSE of the ANN method was 0.61 which is 97.3% and 97.2% more than LSTM+RNN and ANFIS respectively. The low RMSE reduced the MAPE for ANFIS. The variation in RMSE and MAPE is in spite of the equal number of epochs. The error in ANFIS is significantly low. Extrapolation of the load data is also performed for one day ahead and one week ahead forecasting. The results of the extrapolation are shown in Fig. 15-16.

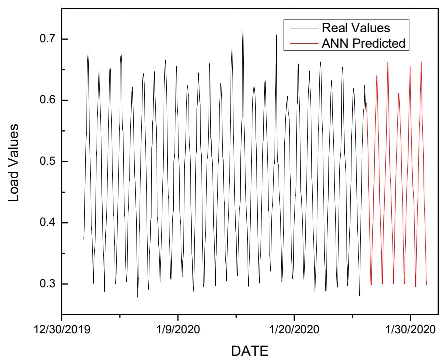

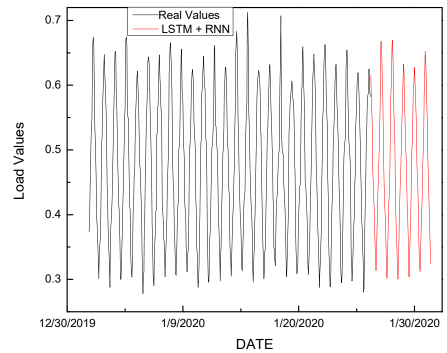

(a)

(b)

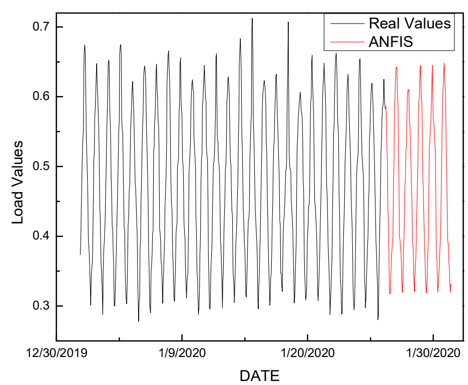

(c)

Fig. 16: Extrapolation for one week ahead a: ANN, b: LSTM+RNN, c: ANFIS

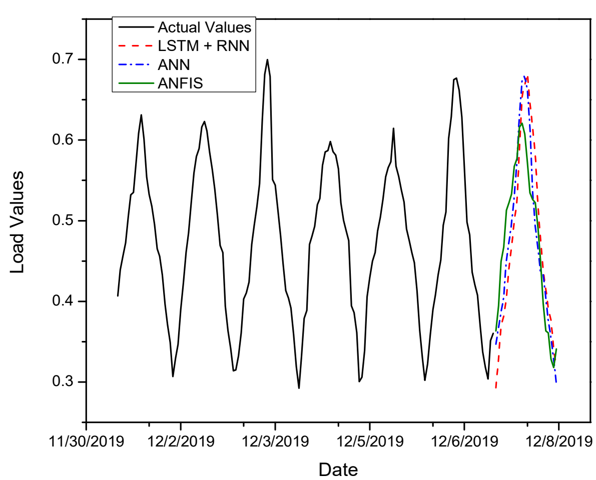

Fig. 17: Extrapolation for one day ahead

From the figure it is perceptible that the forecasting results from ANFIS method is most accurate. The other two methods, i.e., ANN and LSTM+RNN, also give results close to the desired values. The error value obtained from the forecasting method is utilized to feed in for techno-economic optimization using HOMER®. Extrapolation of the load demand is performed to validate the robustness of the analysis.

3.3 Techno-economic analysis of renewable energy systems:

Initially, an analysis of renewable energy combinations accompanied by lead-acid batteries is performed. The techno-economic analysis is performed using the error value obtained from the ANFIS forecasting. The analysis is performed with respect to a currently existing reference diesel generator system. Cost of electricity i.e., the economic parameter, and unmet load i.e., the technical parameter are the two parameters to analyze the techno-economic feasibility of an energy combination.

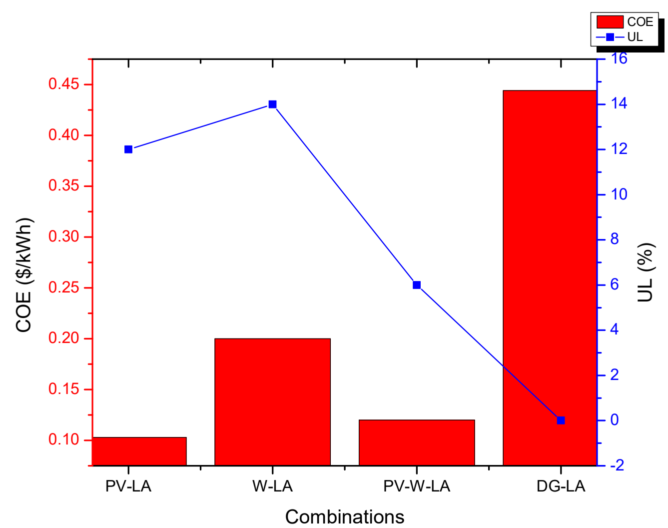

Fig. 18: COE and UL analysis

From Fig. 17 it can be seen that significant amount of load is not met with the renewable energy combinations. For the combination of a wind turbine – lead acid battery the unmet load is 14% which is the highest among all. For the combination of PV-WT-LA and PV-LA, a significant amount of unmet load withstands. For the combination of a diesel generator and lead acid battery, no unmet load is there with a cost of electricity (COE) highest for this combination (i.e., \$0.44/kWh). The COE for PV-LA is the least at \$0.102/kWh. The COEs for PV-WT-LA and WT-LA are \$0.13/kWh & \$0.20/kWh respectively. The COE for the other renewable energy combination is 27.45% to 96.07% more than that of the PV-LA combination. The COE for all the energy combinations is optimal. The unmet load for each energy alternative can be eliminated by increasing the capacity of the alternative. But this will affect economic parameters. The COE would be even higher than the reference DG-LA combination's COE and no optimal solution would be obtained. Therefore, expanding the capacity is not a feasible solution. Hence, to remove the unmet load, an additional diesel generator is appended. The DG will cater power during peak demand hours or when power generation from renewable sources will not be sufficient. Techno-economic analysis and environmental impact assessment are performed again after the addition of the DG. It is followed by performing a MCDM to determine the decided optimal solution.

Techno-economic assessment of the combinations:

The techno-economic parameters of the different energy alternatives are analyzed. The error value obtained from the ANFIS forecasting along with the forecasted data are considered for the techno-economic analysis. The results of the techno-economic parameters are shown in Table 11.

Table 11 :Techno-economic details

	ANFIS			
	COE ($/kWh)	NPC ($)	EE (%)	RF (%)
PV-DG-LA	0.100	5374	21.7	98.7
Wind-DG-LA	0.137	6962	18.1	92.7
PV-Wind-DG-LA	0.167	8236	28.1	99.6
DG-LA	0.444	23738	0	0

From the Table 11 we observe that the economic parameters i.e., COE and NPC are minimum for the PV-DG-LA combination. The COE and NPC are $0.100/kWh and $5374 respectively. The COE of PV-DG-LA is 27.0% to 40.11% lower than the other renewable energy combinations and 77.47% lower than the non-renewable combination. The same trend is observed for the NPC too. The NPC for PV-DG-LA is 22.80% to 34.74% lower than the other renewable combination and 77.36% lower than the non-renewable combination. The excess electricity is the least for WT-DG-LA combination (i.e., 18.1%) and the maximum for the PV-WT-DG-LA combination (i.e., 28.1%). The EE for the PV-DG-LA is 21.7% and no excess electricity is available for the DG-LA combination. Renewable fraction indicates the % of renewable energy in the total power mix. The RF is highest for the PV-WT-DG-LA with 99.6% of renewable energy. The RF for the PV-DG-LA and the WT-DG-LA are 98.7% and 92.7% respectively which is 0.90% and 6.92% lower than that of the PV-WT-DG-LA. To validate the efficacy of the ANFIS method, the other forecasting methods are evaluated under different combinations in Table 12.

Table 12 : Comparison of the ANFIS method with other forecasting methods and without any forecasting

	Without Forecasting				ANN				LSTM+RNN				ANFIS			
	COE ($/kWh)	NPC ($)	EE (%)	RF (%)	COE ($/kWh)	NPC ($)	EE (%)	RF (%)	COE ($/kWh)	NPC ($)	EE (%)	RF (%)	COE ($/kWh)	NPC ($)	EE (%)	RF (%)
PV-DG-LA	0.104	5590	30.8	98.5	0.101	5420	18.6	98.7	0.101	5416	20	98.7	0.100	5374	21.7	98.7
Wind-DG-LA	0.149	6429	26.6	91.1	0.143	6434	16	93	0.14	6256	17.7	92.1	0.137	6962	18.1	92.7
PV-Wind-DG-LA	0.171	9212	38	99.2	0.169	9046	19.3	98.8	0.169	9031	28.5	99.6	0.167	8236	28.1	99.6
DG-LA	0.456	24613	0	0	0.45	24073	0	0	0.448	23997	0	0	0.444	23738	0	0

From Table 12 it is observed that forecasting is beneficial for improving the techno-economic parameters of different energy alternatives. The economic factors i.e., COE & NPC are lesser with forecasting. The COE and NPC decrease by 0.84% to 2.88% and 0.07 to 3.04% respectively with the ANN forecasting. The COE and NPC also lesser by 1.68 to 2.88% and 1.96 to 3.11% respectively relative to LSTM+RNN forecasting. The COE and NPC reduce by 1.68 to 3.84% and 2.71 to 3.86% respectively with ANFIS forecasting. Excess electricity generation is also decreased due to load forecasting. The % of renewable energy is highest for ANFIS forecasting followed by those by LSTM+RNN and ANN. It can also be seen that the PV-DG-LA combination is optimal for all the forecasting approaches. The COE for this alternative is 27 % to 78.07% lesser than other energy combinations. The NPC for the same alternative is 16.41 % to 78.16% lesser than other energy combinations. The EE for the same combination is the lowest. Therefore, the study concludes that implementing load demand forecasting helps for the betterment of efficiency and techno-economic parameters of a decentralized hybrid energy system. To validate the overall sustainability of the system, the environmental impact of the system was also assessed using the capacity obtained by the ANFIS forecasting.

3.4 Environmental Impact Assessment:

The environmental impact of the decentralized hybrid energy system is assessed for both endpoint and midpoint. The midpoint analysis is performed with its 18 characteristics. These 18 characteristics are summed up into three i.e., human health, resource scarcity, and impact on the ecosystem. The results of the endpoint characteristics and midpoint characteristics are illustrated in Figs 13 and 14. The values of the endpoint and midpoint characteristics are shown in Table 13 and 14. The DG-based system is referred to as the base as it is the present existing practice. The different energy combinations are referred to as cases 3.1 to 3.4.

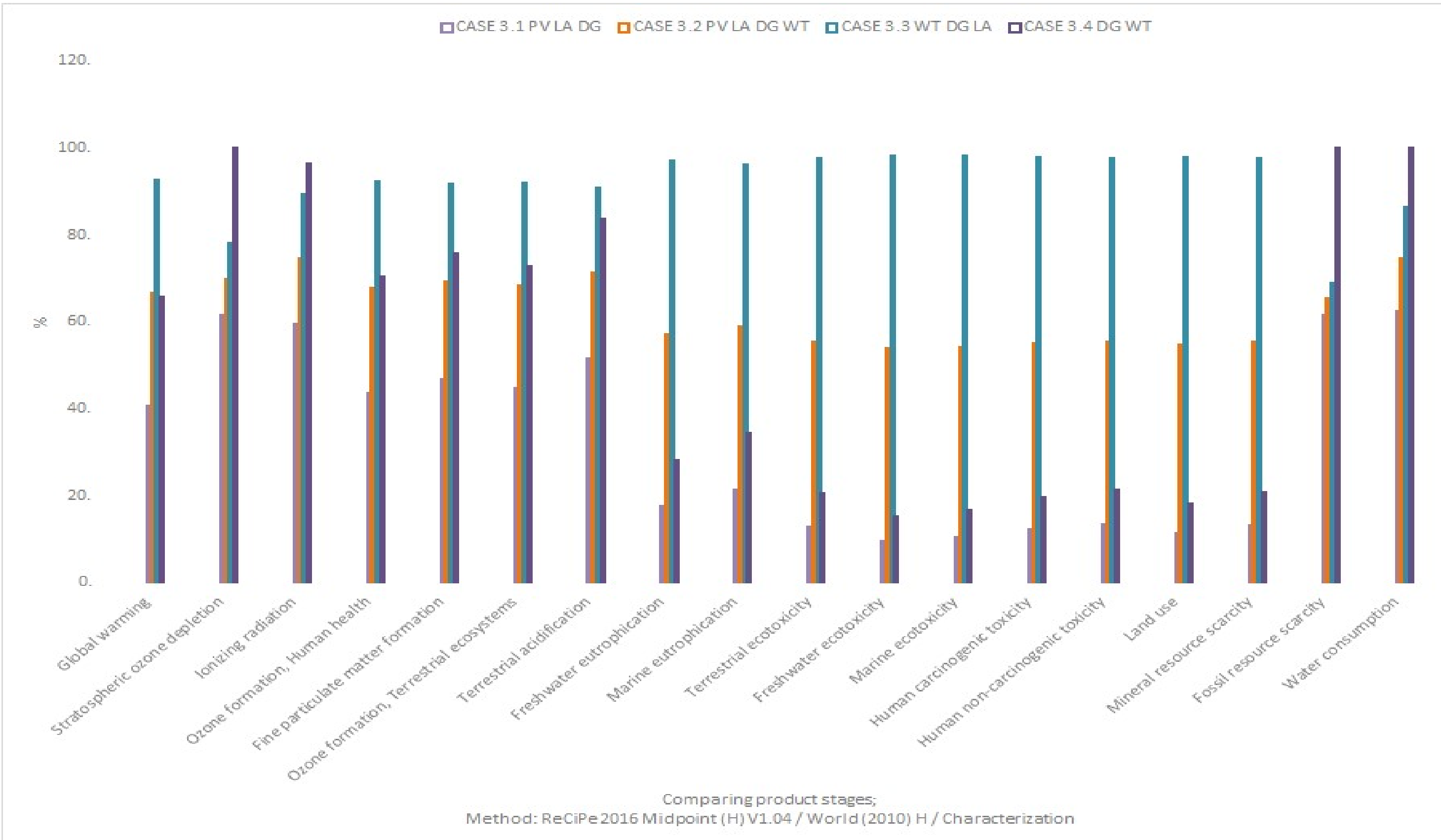

Fig. 19: Midpoint analysis

Table 13: Detailed results of midpoint analysis

Impact category	Unit	CASE 3.1 PV LA DG	CASE 3.2 PV LA DG WT	CASE 3.3 WT DG LA	CASE 3.4 DG WT
Global warming	kg CO2 eq	432866.6	711955.3	989555.8	701942.6
Stratospheric ozone depletion	kg CFC11 eq	0.674868	0.765806	0.854649	1.095903
Ionizing radiation	kBq Co-60 eq	25753.74	32254.13	38665.76	41726.57
Ozone formation, Human health	kg NOx eq	1657.778	2588.838	3514.749	2690.593
Fine particulate matter formation	kg PM2.5 eq	1031.479	1529.248	2023.807	1672.526
Ozone formation, Terrestrial ecosystems	kg NOx eq	1795.897	2744.324	3687.317	2915.438
Terrestrial acidification	kg SO2 eq	2908.633	4015.41	5113.433	4718.688
Freshwater eutrophication	kg P eq	56.46964	183.6238	310.6837	90.78521
Marine eutrophication	kg N eq	4.362085	12.05534	19.73476	7.024569
Terrestrial ecotoxicity	kg 1,4-DCB	1280382	5513305	9748418	2057072
Freshwater ecotoxicity	kg 1,4-DCB	13616.07	77140.74	140747.6	21739.41
Marine ecotoxicity	kg 1,4-DCB	19112.79	100169	181323.5	30562.18
Human carcinogenic toxicity	kg 1,4-DCB	11027.22	50077.28	89071.55	17723.2
Human non-carcinogenic toxicity	kg 1,4-DCB	266788	1115839	1965645	427702.3
Land use	m2a crop eq	31739.47	154044.9	276346.3	50954.08
Mineral resource scarcity	kg Cu eq	1193.629	5041.294	8890.682	1894.543
Fossil resource scarcity	kg oil eq	864776.5	917417.8	967374.2	1404854
Water consumption	m3	5360.031	6386.792	7410.232	8557.409

Figure 19 shows that the combination of PV-DG-LA has the least midpoint impact on the environment. All the characteristics such as global warming, stratospheric ozone depletion, ionizing radiation, ozone formation, finite particulate ozone formation, terrestrial acidification, freshwater eutrophication, marine eutrophication, terrestrial ecotoxicity, marine ecotoxicity, freshwater eutrophication, human carcinogenic and human non-carcinogenic, land use, mineral resource scarcity, fossil resource scarcity and water consumption are lesser for PV-DG-LA combination. Values of these characteristics are 39.2%, 11.87%, 20.15%, 35.96%, 32.54%, 34.56%, 27.56%, 69.24%, 63.81%, 76.77%, 82.34%, 80.91%, 77.98%, 76.09%, 79.39%, 76.32%, 5.73% and 16.07% lesser respectively for this combination than those of the PV-Wind-DG-LA. A similar trend is observed for the Wind-DG-LA combination

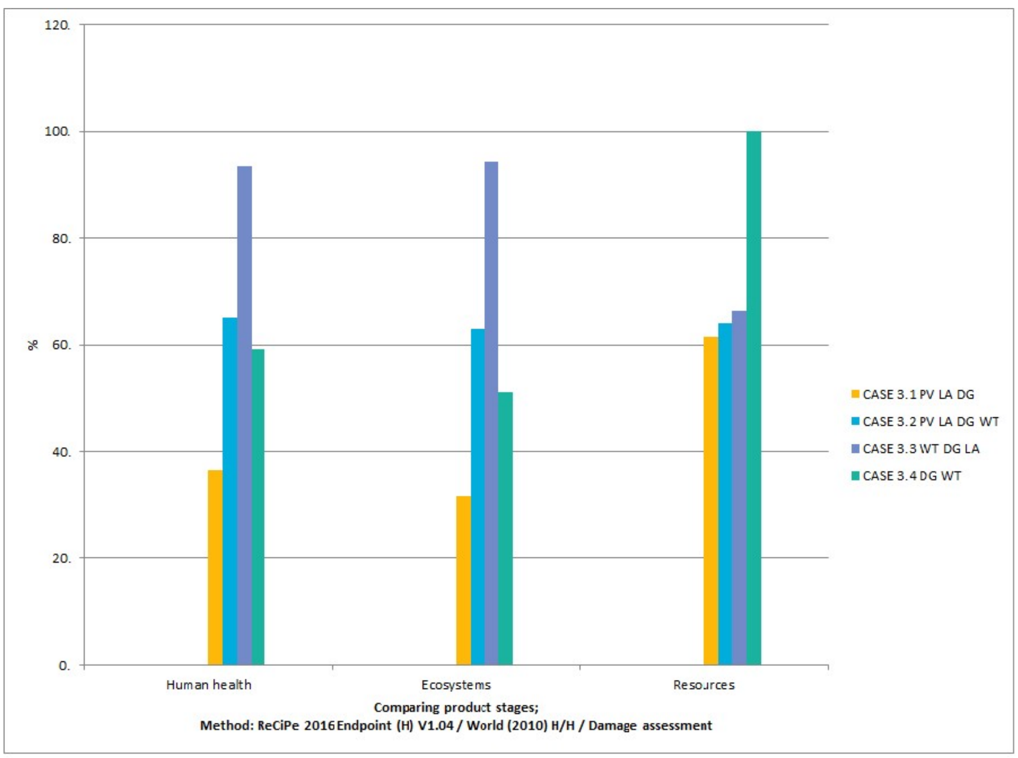

Fig. 20 Endpoint analysis (Environmental impact assessment)

Table 14: Data of endpoint analysis

Damage category	Unit	Case 3.1 (PV-DG-LA)	Case 3.2 (PV-WT-LA)	Case 3.3 (WT-DG-LA)	Case 3.4 (DG-LA)
Resources	USD2013	386120.8	401586.4	415863.3	627329.2
Ecosystems	species.yr	0.002438	0.004855	0.007267	0.003947
Human health	DALY	1.14984	2.046605	2.939991	1.86258

The endpoint analysis as shown in Fig. 20 justifies the midpoint analysis result. The human health impact for this combination is 43.81% and 30.38% lesser respectively as compared to other two combinations. Other two categories such as ecosystem impact and resource scarcity follow the similar trend. The environmental impact assessment shows that the combination of PV-DG-LA for the ANFIS forecasting method is the environmentally optimal solution.

According to the overall analysis PV-DG-LA combination is an economic and environmentally benign solution. However, PV-Wind-DG-LA has the maximum renewable share. On the other hand, the technical performance factor, i.e., EE is least in the Wind-DG-LA combination. Therefore, obtaining a simultaneous optimum techno-economic and environmentally benign solution is not obtained. Hence, to decide a practically acceptable optimum solution a MCDM approach is used.

3.5. MCDM and sensitivity analysis:

The TOPSIS-MCDM is used to select the feasible optimum combination by considering the decided weights of the sustainability criteria. The decided sustainability criteria are COE, NPC, EE, renewable fraction, and endpoint parameters of the LCA. The scale value is considered for the environmental impact assessment parameters. The decision-making matrix is shown in Table 15.

Table 15: Decision matrix

Combinations	COE ($/kWh)	NPC ($)	Excess Electricity (%)	Human health	Ecosystem	Resource scarcity	Renewable Fraction (%)
PV-DG-LA	0.1	5374	21.7	2	2	3	98.7
PV-WT-DG-LA	0.167	8236	28.1	3	4	4	99.6
WT-DG-LA	0.137	6962	18.1	4	5	4	92.7

The equal weights are considered for this decided criteria. The decision-making analysis result is shown in Fig. 21.

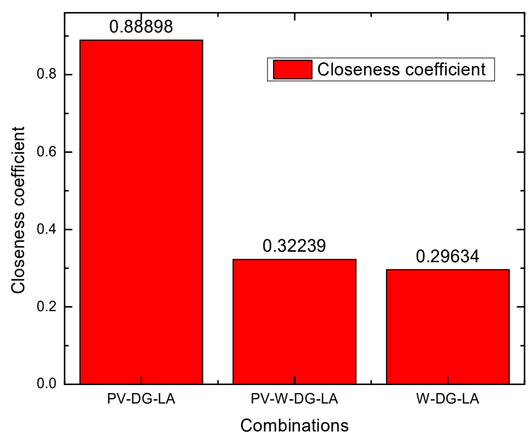

Fig. 21 Closeness coefficient of the combinations

A more detailed analysis result is shown in Table 15-16.

According to Fig. 16 the closeness coefficient of the PV-DG-LA combination is maximum followed by the PV-W-DG-LA and W-DG-LA combinations. This PV-DG-LA combination holds the 1st rank. To evaluate the robustness of the obtained solution the VIKOR-MCDM method is performed as a sensitivity analysis. The analysis is performed on the basis of equal weights of the decided criteria. The analysis result is shown in Table 8. The detailed analysis results are shown in Table 16.

Table 16: Sensitivity analysis

Combinations	SI	RI	QI	RANK
PV-DG-LA	0.06001	0.06001	0	1
PV-WT-DG-LA	0.86128	0.1667	1	3
WT-DG-LA	0.68465	0.1667	0.889781	2
SI(-),RI(-)	0.861283	0.1667		
SI(*), RI(*)	0.060012	0.060012		

The sensitivity analysis shows that the combination of PV-DG-LA is the acceptable feasible optimal solution. This sensitivity analysis shows that the obtained solution is robust. According to the integrated methodology analysis result the combination of PV-DG-LA is techno-economically optimal and environmentally solution under ANFIS forecasting method as compared to other alternatives.

Chapter-4

Conclusion and future scope

4.1 Conclusion:

This study is aimed to find a combined techno-economically optimal and environmentally sustainable decentralized hybrid energy solution integrated with forecasting of load. In this study, three different forecasting methods, i.e., normal forecasting (ANN), hybrid forecasting (LSTM+RNN) and fuzzy forecasting (ANFIS) are compared to select the best forecasting method. Both the short-term and the medium-term forecasting methods are performed in this study. With the forecasted load and corresponding error value, subsequently techno-economic optimization and comprehensive environmental impact assessment using LCA method is performed. As the corresponding best solutions for techno-economic and environmental performance are different, finally the MCDM approach is used to decide an acceptable optimum combination on the basis of decided weights of these criteria.

The analysis results show that the ANFIS forecasting is the most accurate load forecasting approach. The error value is 3.3% and 6.8% lesser than those by the other considered forecasting methods. By considering this result three major sustainability assessment indices, i.e., technical factors, economic and environmental impact are assessed in this study. According to this analysis economic factors and the environmental impact assessment are least for the PV-DG-LA combination (COE-$0.100/kWh, NPC- $5375, human health- 1.14 DALY, ecosystems- 0.002 species.yr and resources- 386120 USD2013 respectively). However, the technical factor (EE) is not minimum for this combination. It is minimum for Wind-DG-LA combination (approximately 18.6%). Finally, PV-DG-LA combination is decided as techno-economically feasible (COE-$0.100/kWh, NPC-$5374 and EE-21.7%) and environmentally sustainable solution through MCDM approach. The sensitivity analysis shows that the obtained solution is robust. This integrated methodology shows that the fuzzy-based forecasting approach is more accurate. It helps to improve techno-economic and environmental performance of the combinations by minimizing the load uncertainty. In future analysis the sensitivity analysis may perform to evaluate the robustness of the system. The result may vary with the change of location but the proposed integrated methodology is novel and generic.

4.2 Future Scope:

- The uncertainty of natural resources can be predicted and integrated with load forecasting improving the sustainability of the proposed standalone energy system. Several social and geographical factors play an important role in changing the load pattern. Integrating this with the load forecasting will improve the accuracy of the load forecasting further.
- Due to the intermittency of renewable power generation and uncertainty in load demand excess electricity is inevitable. In most hybrid renewable energy systems, the excess electricity is dumped. The excess electricity can be utilized by transforming it to some other forms. Future analysis may be carried out with such systems for a better overall sustainability.
- Financial risk assessment of the proposed hybrid energy system can also be performed.
- The social aspect analysis of the proposed hybrid energy system can be performed.

References:

[1] Das S, Pradhan S, De S. Multi criteria decision making for the most suitable combination of energy resources for a decentralized hybrid energy solution with green hydrogen as the storage option. Energy Convers Manag 2023;285:117028. https://doi.org/10.1016/j.enconman.2023.117028.

[2] Adewuyi OB, Kiptoo MK, Adebayo IG, Adewuyi OI, Senjyu T. Techno-economic analysis of robust gas-to-power distributed generation planning for grid stability and environmental sustainability in Nigeria. Sustain Energy Technol Assessments 2023;55:102943. https://doi.org/10.1016/j.seta.2022.102943.

[3] Das S, De S. MCDM for simultaneous optimum economy, investment risk and environmental impact for distributed renewable power: Demonstration with an Indian village data. Energy Convers Manag 2023;277:116631. https://doi.org/10.1016/j.enconman.2022.116631.

[4] Das S, Ray A, De S. Optimum combination of renewable resources to meet local power demand in distributed generation: A case study for a remote place of India. Energy 2020;209:118473. https://doi.org/10.1016/j.energy.2020.118473.

[5] Kumar P, Pal N, Sharma H. Optimization and techno-economic analysis of a solar photo-voltaic/biomass/diesel/battery hybrid off-grid power generation system for rural remote electrification in eastern India. Energy 2022;247:123560. https://doi.org/10.1016/j.energy.2022.123560.

[6] Khan FA, Pal N, Saeed SH. Optimization and sizing of SPV/Wind hybrid renewable energy system: A techno-economic and social perspective. Energy 2021;233:121114. https://doi.org/10.1016/j.energy.2021.121114.

[7] Aly HHH. A proposed intelligent short-term load forecasting hybrid models of ANN, WNN and KF based on clustering techniques for smart grid. Electr Power Syst Res 2020;182:106191. https://doi.org/10.1016/j.epsr.2019.106191.

[8] Lebotsa ME, Sigauke C, Bere A, Fildes R, Boylan JE. Short term electricity demand forecasting using partially linear additive quantile regression with an application to the unit commitment problem. Appl Energy 2018;222:104–18. https://doi.org/10.1016/j.apenergy.2018.03.155.

[9] Zhang W, Maleki A, Rosen MA, Liu J. Sizing a stand-alone solar-wind-hydrogen

energy system using weather forecasting and a hybrid search optimization algorithm. Energy Convers Manag 2019;180:609–21. https://doi.org/10.1016/j.enconman.2018.08.102.

[10] Peng LL, Fan GF, Yu M, Chang YC, Hong WC. Electric Load Forecasting based on Wavelet Transform and Random Forest. Adv Theory Simulations 2021;4:1–11. https://doi.org/10.1002/adts.202100334.

[11] Li K, Huang W, Hu G, Li J. Ultra-short term power load forecasting based on CEEMDAN-SE and LSTM neural network. Energy Build 2023;279. https://doi.org/10.1016/j.enbuild.2022.112666.

[12] Chen Y, Tan H. Short-term prediction of electric demand in building sector via hybrid support vector regression. Appl Energy 2017;204:1363–74. https://doi.org/10.1016/j.apenergy.2017.03.070.

[13] Chen JF, Wang WM, Huang CM. Analysis of an adaptive time-series autoregressive moving-average (ARMA) model for short-term load forecasting. Electr Power Syst Res 1995;34:187–96. https://doi.org/10.1016/0378-7796(95)00977-1.

[14] Fang X, Zhang W, Guo Y, Wang J, Wang M, Li S. A Novel Reinforced Deep RNN-LSTM Algorithm: Energy Management Forecasting Case Study. IEEE Trans Ind Informatics 2022;18:5698–704. https://doi.org/10.1109/TII.2021.3136562.

[15] Ghenai C, Al-Mufti OAA, Al-Isawi OAM, Amirah LHL, Merabet A. Short-term building electrical load forecasting using adaptive neuro-fuzzy inference system (ANFIS). J Build Eng 2022;52:104323. https://doi.org/10.1016/j.jobe.2022.104323.

[16] Barman M, Dev Choudhury NB, Sutradhar S. A regional hybrid GOA-SVM model based on similar day approach for short-term load forecasting in Assam, India. Energy 2018;145:710–20. https://doi.org/10.1016/j.energy.2017.12.156.

[17] Xiao X, Mo H, Zhang Y, Shan G. Meta-ANN – A dynamic artificial neural network refined by meta-learning for Short-Term Load Forecasting. Energy 2022;246:123418. https://doi.org/10.1016/j.energy.2022.123418.

[18] Jin N, Yang F, Mo Y, Zeng Y, Zhou X, Yan K, et al. Highly accurate energy consumption forecasting model based on parallel LSTM neural networks. Adv Eng Informatics 2022;51:101442. https://doi.org/10.1016/j.aei.2021.101442.

[19] Goh HH, He B, Liu H, Zhang D, Dai W, Kurniawan TA, et al. Multi-Convolution Feature Extraction and Recurrent Neural Network Dependent Model for Short-

Term Load Forecasting. IEEE Access 2021;9:118528–40. https://doi.org/10.1109/ACCESS.2021.3107954.

[20] Malik P, Awasthi M, Sinha S. Techno-economic and environmental analysis of biomass-based hybrid energy systems: A case study of a Western Himalayan state in India. Sustain Energy Technol Assessments 2021;45:101189. https://doi.org/10.1016/j.seta.2021.101189.

[21] Khan FA, Pal N, Saeed SH, Yadav A. Modelling and techno-economic analysis of standalone SPV/Wind hybrid renewable energy system with lead-acid battery technology for rural applications. J Energy Storage 2022;55:105742. https://doi.org/10.1016/j.est.2022.105742.

[22] Das S, De S. Technically efficient , economic and environmentally benign hybrid decentralized energy solution for an Indian village : Multi criteria decision making approach. J Clean Prod 2023;388:135717. https://doi.org/10.1016/j.jclepro.2022.135717.

[23] Kumar P, Pal N, Sharma H. Techno-economic analysis of solar photo-voltaic/diesel generator hybrid system using different energy storage technologies for isolated islands of India. J Energy Storage 2021;41:102965. https://doi.org/10.1016/j.est.2021.102965.

[24] Das S, Ray A, De S. Comparative analysis of storage modules under different dispatch strategies for an optimum decentralized hybrid energy solution: a case study of a remote Indian village. Clean Technol Environ Policy 2022;24:2495–515. https://doi.org/10.1007/s10098-022-02330-0.

[25] Murugaperumal K, Srinivasn S, Satya Prasad GRKD. Optimum design of hybrid renewable energy system through load forecasting and different operating strategies for rural electrification. Sustain Energy Technol Assessments 2020;37:100613. https://doi.org/10.1016/j.seta.2019.100613.

[26] Salameh T, Ghenai C, Merabet A, Alkasrawi M. Techno-economical optimization of an integrated stand-alone hybrid solar PV tracking and diesel generator power system in Khorfakkan, United Arab Emirates. Energy 2020;190:116475. https://doi.org/10.1016/j.energy.2019.116475.

[27] Kumar R, Channi HK. A PV-Biomass off-grid hybrid renewable energy system (HRES) for rural electrification: Design, optimization and techno-economic-environmental analysis. J Clean Prod 2022;349. https://doi.org/10.1016/j.jclepro.2022.131347.

[28] India G of. Indian Village Directory n.d. https://villageinfo.in/odisha.html (accessed February 11, 2023).
[29] Government of Odisha. Mayurbhanj. 2020 n.d.
[30] Pradhan A. Odisha: Hamlet in Droupadi Murmu's ancestral village still does not have electricity. Times of India 2022.
[31] Suffian M. NDA presidential candidate Droupadi Murmu's village to get power for the first time. India Today 2022. https://www.indiatoday.in/india/story/nda-presidential-candidate-droupadi-murmu-odisha-electricity-1966930-2022-06-26.
[32] Idoko L, Anaya-Lara O, McDonald A. Enhancing PV modules efficiency and power output using multi-concept cooling technique. Energy Reports 2018;4:357–69. https://doi.org/10.1016/j.egyr.2018.05.004.
[33] Salameh T, Sayed ET, Abdelkareem MA, Olabi AG, Rezk H. Optimal selection and management of hybrid renewable energy System: Neom city as a case study. Energy Convers Manag 2021;244:114434. https://doi.org/10.1016/j.enconman.2021.114434.
[34] NASA. "NASA weather report," 2020. n.d.
[35] Das S, De S. Technically efficient, economic and environmentally benign hybrid decentralized energy solution for an Indian village: Multi criteria decision making approach. J Clean Prod 2023;388:135717. https://doi.org/10.1016/j.jclepro.2022.135717.
[36] Ma T, Javed MS. Integrated sizing of hybrid PV-wind-battery system for remote island considering the saturation of each renewable energy resource. Energy Convers Manag 2019;182:178–90. https://doi.org/10.1016/j.enconman.2018.12.059.
[37] Edwan TA, Tahat A, Hammouri S, Hashem L, Da'boul L. An intelligent and automated approach for smart minimarkets. Int J Comput Intell Syst 2020;13:852–63. https://doi.org/10.2991/ijcis.d.200611.001.
[38] Kimura N, Yoshinaga I, Sekijima K, Azechi I, Baba D. Convolutional neural network coupled with a transfer-learning approach for time-series flood predictions. Water (Switzerland) 2020;12. https://doi.org/10.3390/w12010096.
[39] Massaoudi M, Chihi I, Sidhom L, Trabelsi M, Refaat SS, Oueslati FS. Performance Evaluation of Deep Recurrent Neural Networks Architectures: Application to PV Power Forecasting. 2nd Int Conf Smart Grid Renew Energy, SGRE 2019 - Proc 2019. https://doi.org/10.1109/SGRE46976.2019.9020965.

[40] Subbiah SS, Chinnappan J. Deep learning based short term load forecasting with hybrid feature selection. Electr Power Syst Res 2022;210:108065. https://doi.org/10.1016/j.epsr.2022.108065.

[41] Apaydin H, Feizi H, Sattari MT, Colak MS, Shamshirband S, Chau KW. Comparative analysis of recurrent neural network architectures for reservoir inflow forecasting. Water (Switzerland) 2020;12:1–18. https://doi.org/10.3390/w12051500.

[42] Syed D, Abu-Rub H, Ghrayeb A, Refaat SS. Household-Level Energy Forecasting in Smart Buildings Using a Novel Hybrid Deep Learning Model. IEEE Access 2021;9:33498–511. https://doi.org/10.1109/ACCESS.2021.3061370.

[43] Muhuri PS, Chatterjee P, Yuan X, Roy K, Esterline A. Using a long short-term memory recurrent neural network (LSTM-RNN) to classify network attacks. Inf 2020;11:1–21. https://doi.org/10.3390/INFO11050243.

[44] Sokhansanj A, Zabihi M. Remarkable dynamic adsorption of Hg2+ ions on the magnetic MOF nanocomposite (CuNi-BTC@Fe3O4): Experimental and modeling using GA+CFD+ANFIS method. J Clean Prod 2022;371:133304. https://doi.org/10.1016/j.jclepro.2022.133304.

[45] Hai T, Wang D, Muranaka T. An improved MPPT control-based ANFIS method to maximize power tracking of PEM fuel cell system. Sustain Energy Technol Assessments 2022;54:102629. https://doi.org/10.1016/j.seta.2022.102629.

[46] Introduction to LCA with SimaPro Colophon 2013.

[47] Wernet G, Bauer C, Steubing B, Reinhard J, Moreno-Ruiz E, Weidema B. The ecoinvent database version 3 (part I): overview and methodology. Int J Life Cycle Assess 2016;21:1218–30. https://doi.org/10.1007/s11367-016-1087-8.

[48] Aberilla JM, Gallego-Schmid A, Stamford L, Azapagic A. Design and environmental sustainability assessment of small-scale off-grid energy systems for remote rural communities. Appl Energy 2020;258:114004. https://doi.org/10.1016/j.apenergy.2019.114004.

[49] Kabir MR, Rooke B, Dassanayake GDM, Fleck BA. Comparative life cycle energy, emission, and economic analysis of 100 kW nameplate wind power generation. Renew Energy 2012;37:133–41. https://doi.org/10.1016/j.renene.2011.06.003.

[50] Jana K, De S. Techno-economic evaluation of a polygeneration using agricultural residue - A case study for an Indian district. Bioresour Technol 2015;181:163–73.

https://doi.org/10.1016/j.biortech.2015.01.060.

[51] Mark Goedkoop, Michiel Oele, Marisa Vieira, Jorrit Leijting, Tommie Ponsioen EM. SimaPro Tutorial Colophon 2014.

[52] Ray A, Jana K, Assadi M, De S. Distributed polygeneration using local resources for an Indian village: multiobjective optimization using metaheuristic algorithm. Clean Technol Environ Policy 2018;20:1323–41. https://doi.org/10.1007/s10098-018-1562-y.

List of Symbols:

Abbreviations:

ANN	Artificial Neural Network
ARIMA	Auto-Regression Integrated Moving Average
ANFIS	Adaptive Neuro Fuzzy Interference System
CNN	Convolution Neural Network
COE	Cost of electricity (US$)
CRF	Capital Recovery Factor
DG	Diesel Generator
EE	Excess electricity
FU	Functional unit
HOMER	Hybrid Optimization of Multiple Electric Renewable
LCA	Life Cycle Assessment
LA	Lead acid
LF	Load following
Li-ion	Lithium-ion battery
LSTM	Long Short-Term Memory
MCDM	Multi-Criteria Decision Making
MAPE	Mean absolute percentage error
MSE	Mean square error
NPC	Net Present Cost ($)
O & M	Cost of system's operation and maintenance ($/kW/y)
PV	Photovoltaic module
RMSE	Root Mean Square Error
RNN	Recurrent Neural Network
SDG	Sustainable Development Goals
SVM	Support Vector Machine
TOPSIS	Technique for Order of Preference by Similarity to Ideal Solution
UL	Unmet load
VIKOR	VIekriterijumsko KOmpromisno Rangiranje
ZB	Zinc Bromide

Nomencleature:

A	Area covered by the bldes of the turbine
C_A	Annualized cost ($)
C_i	Capital cost (US$)
C_R	Cost of replacement (US$)
$C_{O\&M}$	Operation and maintenance cost (US$)
C_{fy}	Fuel cost (US$/L)
C_{NPC}	Net present cost
c_p	Benz's constant
$S_{bat,cm}$	Maximum energy in storage modules (kWh)
DGC	Coefficient of fuel curve intercept (Units/h/kW)
f_{pv}	Derating factor (%)
H_h	Hub height of wind turbine (m)
H_{ref}	Hub height of anemometer(m)
I_{STC}	Solar radiation at standard situation (W per sq. m per day)
N_{batt}	Minimum battery requirement
N_{PV}	Number of solar modules
N_{WT}	Total number of wind turbines
P_{Peak}	Peak time power
P_{PV}	PV module's output power in kW
P_m	Maximum power generated from wind turbine
$P_{pv,stc}$	PV module's output power in standard temperature condition in kW
P_W	power produced by wind turbine (kW)
$Pr\ (t)$	Rated power of wind turbine
P_{conv}	Power of inverter
T_a	Ambient temperature. (°C)
t_c	PV module's cell temperature (°C)
V_{rw}	Rated wind velocity at hub height (m per s)
$Y_{pv,stc}$	Rated capacity of module at standard condition

Greek Letters:

α_c	Maximum charging rate
σ	Self-discharge percentage
η	Efficiency
γ	Hellman constant

List of publications produced from the thesis submitted by Risav Dutta

International Journal

1. Dutta R, Das S, De S. Multi criteria decision making with machine-learning based load forecasting methods for techno-economic and environmentally sustainable distributed hybrid energy solution. Energy Conversion and Management (Elsevier) (Under second revision)

International Conference

1. Das S, Dutta R, Chakraborty S, De S. Techno-economic assessment and Sizing optimization of combined heat and power system: A case study of Rural India. Proceedings of the International Conference on Chemical Engineering Innovation & Sustainability (ICEIS 2023), Organized by Jadavpur University, Kolkata, India.